From MOLECULAR MEDICINE AND SURGERY
Karolinska Institutet, Stockholm, Sweden

PATHWAYS CONTROLLING METABOLIC AND HYPERTROPHIC RESPONSES IN SKELETAL MUSCLE

Isabelle Riedl

Karolinska Institutet

Stockholm 2015

Published by Karolinska Institutet.
Printed by Karolinska Universityservice US-AB.

ISBN 978-91-7549-973-4

Pathways controlling metabolic and hypertrophic responses in skeletal muscle

THESIS FOR DOCTORAL DEGREE (Ph.D.)

by

Isabelle Riedl

Principal Supervisor:
Professor Juleen R. Zierath
Karolinska Institutet
Department of Molecular Medicine and Surgery
Department of Physiology and Pharmacology
Section of Integrative Physiology

Co-supervisor:
Dr. Megan E. Osler
Karolinska Institutet
Department of Molecular Medicine and Surgery
Section of Integrative Physiology

Opponent:
Professor Jørgen Jensen
Norwegian School of Sport Sciences
Department of Physical Performance

Examination Board:
Professor Eva Jansson
Karolinska Institutet
Department of Laboratory Medicine

Professor Lars Larsson
Karolinska Institutet
Department of Physiology and Pharmacology

Professor Tore Bengtsson
Stockholm University
Department of Molecular Biosciences
The Wenner-Gren Institute

"*What is that feeling when you're driving away from people and they recede on the plain till you see their specks dispersing? – it's the too-huge world vaulting us, and it's good-by. But we lean forward to the next crazy venture beneath the skies.*"

Jack Kerouac – On the Road

ABSTRACT

Skeletal muscle displays an extensive capacity to adapt to a wide range of metabolic and mechanical stressors. As an insulin-sensitive and exercise-responding tissue, it plays a key role in the context of therapeutic interventions targeting metabolic diseases including type 2 diabetes (T2D) and obesity. The aim of this thesis was to gain mechanistic insight into the adaptive response of skeletal muscle to different genetic and environmental stressors by using *in vitro* and *in vivo* models.

This work, with a unique *in vitro* longitudinal model, has allowed the broadening of knowledge about how skeletal muscle adapts to weight-loss surgery. Notably, glucose storage as glycogen, but not fatty acid oxidation was improved in myotubes derived from skeletal muscle biopsies from patients who underwent gastric bypass surgery. Potential new targets mediating the metabolic effects of surgery in skeletal muscle include proline-rich Akt substrate of 40kDa (PRAS40).

By genotyping a cohort of individuals with either normal glucose tolerance (NGT), impaired glucose tolerance (IGT) or T2D, the impact of the ACTN3 R577X polymorphism on metabolic disease was evaluated. A higher proportion of T2D patients with the homozygous null allele (577XX) was detected, but no further association with clinical parameters could be established. Rather, the presence of the 577XX genotype is associated with increased mRNA levels of genes involved in structural integrity of skeletal muscle.

Surgical removal of synergistic skeletal muscle to induce functional overload and hypertrophy in the plantaris muscle of genetically modified mice addressed whether the γ3 subunit of the energy cell sensor AMPK plays a role in skeletal muscle remodeling in the context of hypertrophy. Following a 14-day functional overload, skeletal muscle of transgenic (R225Q), knockout and wild-type mouse models underwent a similar hypertrophic response, as demonstrated by functional, transcriptional and signaling data. Due to increased mass at baseline, the plantaris muscle of R225Q mice underwent a smaller change in weight gain. Overall, this work demonstrates that the AMPK γ3 isoform is dispensable for skeletal muscle hypertrophy.

Collectively, the results presented in this thesis provide new information about the remodeling capacity of skeletal muscle in response to the above-mentioned stressors. Environmental and genetic factors affect skeletal muscle by modifying local signaling pathways and inducing changes in energy metabolism, subsequently impacting whole-body energy homeostasis.

LIST OF SCIENTIFIC PAPERS

I. Emmani B. M. Nascimento, **Isabelle Riedl**, Lake Qunfeng Jiang, Sameer S. Kulkarni, Erik Näslund and Anna Krook. Enhanced glucose metabolism in cultured human skeletal muscle after Roux-en-Y gastric bypass surgery. Surgery for Obesity and Related Diseases DOI: http://dx.doi.org/10.1016/j.soard.2014.11.001, 2014.

II. **Isabelle Riedl**, Megan E. Osler, Boubacar Benziane, Alexander V. Chibalin and Juleen R. Zierath. Association of the ACTN3 R577X polymorphism with glucose tolerance and gene expression of sarcomeric proteins in human skeletal muscle. Physiological Reports 3 e12314, DOI: 10.14814/phy2.12314, 2015.

III. **Isabelle Riedl**, Megan E. Osler, Marie Björnholm, Brendan Egan, Gustavo A. Nader, Alexander V. Chibalin and Juleen R. Zierath. AMPK γ3 is dispensable for skeletal muscle hypertrophy. In manuscript.

CONTENTS

LIST OF ABBREVIATIONS

4E-BP1	4E-binding protein 1
ACC	Acetyl-CoA carboxylase
ACE	Angiotensin-converting enzyme
ACSL1	Acyl-CoA synthetase long-chain family member 1
ACTN	Alpha-actinin
ADP	Adenosine diphosphate
AICAR	5-Aminoimidazole-4-carboxamide ribonucleotide
Akt	Protein kinase B
AMP	Adenosine monophosphate
AMPK	5-AMP-activated protein kinase
ANOVA	Analysis of variance
AS160	Akt-substrate of 160 kDa
ATP	Adenosine triphosphate
BMI	Body mass index
CaMKII	Ca^{2+}-calmodulin-dependent protein kinase II
cDNA	Complementary DNA
COX2	Cytochrome C oxidase subunit 2
DMEM	Dulbecco modified eagle medium
EDL	Extensor digitorum longus
EDTA	Ethylenediaminetetraacetic acid
ELISA	Enzyme-linked immunosorbent assay
FOXO3	Forkhead-box O3
GLP-1	Glucagon-like peptide 1

HbA1c	Glycosylated hemoglobin
HOMA-IR	Homeostasis model assessment – estimated insulin resistance
HWE	Hardy-Weinberg equilibrium
IGF1	Insulin-like growth factor 1
IGT	Impaired glucose tolerance
IKK	IκB kinase
IL6	Interleukin-6
IL8	Interleukin-8
IRS	Insulin receptor substrate
JNK	c-Jun N-terminal kinase
LC3	Microtubule-associated protein 1 light chain 3
Mafbx	F-box protein 32
mRNA	Messenger RNA
mTORC	Mammalian target of rapamycin complex
MyHC	Myosin heavy chain
MyoD	Myogenic differentiation 1
NDUFB8	NADH dehydrogenase 1 beta subcomplex 8
NFAT	Nuclear factor of activated T-cells
NGT	Normal glucose tolerance
Murf1	Tripartite motif-containing 63
OGTT	Oral glucose tolerance test
p62	Sequestosome 1
p70S6k	Phosphoprotein 70 ribosomal protein S6 kinase
PAX	Paired-box

PDLIM	PDZ and LIM domain
PGC1α	Peroxisome proliferator-activated receptor gamma, coactivator 1 alpha
PI3K	Phosphoinositide 3-kinase
PKC	Protein kinase C
PRAS40	Proline-rich Akt substrate of 40 kDa
PRKAG	AMP-activated protein kinase gamma subunit
Raptor	Regulatory-associated protein of mTOR
RPS6	Ribosomal protein S6
RT-qPCR	Real-time quantitative polymerase chain reaction
RYGB	Roux-en-Y gastric bypass surgery
SDS-PAGE	Sodium dodecyl sulfate-polyacrylamide gel electrophoresis
SEM	Standard error of the mean
SOCS3	Suppressor of cytokine signaling 3
T2D	Type 2 diabetes
TBST	Tris buffered saline-Tween
TNFα	Tumor necrosis factor α
TSC	Tuberous sclerosis complex
VO_2max	Maximal oxygen uptake
WHO	World Health Organisation

1 INTRODUCTION

1.1 LIFESTYLE-RELATED METABOLIC DISEASES

1.1.1 Type 2 diabetes and obesity

Lifestyle-related metabolic disorders such as obesity and type 2 diabetes (T2D) currently place an increasing global burden on public health and the economy. These afflictions mainly result from the synergistic effect of genetic and environmental factors, including reduced physical activity and increased caloric intake, and are exacerbated by population aging (Danaei *et al.*, 2011). Progressively, over-nutrition and a sedentary lifestyle leads to obesity, as defined by an excessive accumulation of body fat that presents a risk for health (WHO, 2015). Worldwide, 39% of the adult population is overweight and 13% is obese (WHO, 2015). Obesity in human adults is diagnosed using body mass index (BMI, kg/m^2) (WHO, 2015). Waist circumference and waist-to-hip ratio have also emerged as complementary clinical tools to diagnose obesity and cardiometabolic risk (Ashwell *et al.*, 2012; WHO, 2015). An individual is considered overweight with a BMI of 25 kg/m^2 to 29.9 kg/m^2, obese with a BMI of >30 kg/m^2, and extremely obese with a BMI >40 kg/m^2. As obesity develops, changes in whole-body glucose and lipid metabolism occur and ultimately lead to insulin resistance. Together, obesity and insulin resistance are potent drivers of the metabolic syndrome, a constellation of risk factors that synergistically increase the risk for cardiovascular disease, T2D and mortality (Moller & Kaufman, 2005).

More than 170 million individuals are estimated to have T2D and by 2030, this number is expected to increase to 366 million (Wild *et al.*, 2004). T2D is a chronic, non-communicable disease characterized by abnormally increased blood glucose concentration (hyperglycemia) resulting from an incapacity of the body to efficiently utilize insulin to reduce blood glucose levels (WHO, 2015). Impaired glucose tolerance (IGT) often precedes overt T2D. IGT and T2D are clinically diagnosed using an oral glucose tolerance test (OGTT; Table 1) (IDF, 2006).

Table 1: 2006 WHO recommendations for the diagnostic criteria for impaired glucose tolerance and type 2 diabetes.

	Fasting blood glucose	2 hr blood glucose
Impaired glucose tolerance	<7.0	≥7.8 and <11.1
Type 2 diabetes	≥7.0	≥11.1

Units are mmol/l.

1.1.2 Strategies to improve metabolic health

1.1.2.1 Lifestyle interventions

The current recommended treatment for obesity and T2D include lifestyle intervention through physical activity and diet in order to reduce body weight and achieve better glycemic control (Boule *et al.*, 2001; Tuomilehto *et al.*, 2001; Knowler *et al.*, 2002; Colberg *et al.*, 2010; Goodpaster *et al.*, 2010). In insulin resistant people with T2D, the ability to switch between energy substrates for energy production, coined "*metabolic flexibility"* (Brooks & Mercier, 1994), is impaired. The relative contribution of energy substrates, including carbohydrates and lipids, is modulated by exercise intensity. Exercise training results in the ability to switch fuel sources and improves metabolic flexibility (Fig. 1). Updated exercise prescription guidelines recommend a combination of both endurance and resistance-based exercise in order to tackle T2D (Colberg *et al.*, 2010). Finally, new strategies for exercise prescription in the context of metabolic disease include low volume, high intensity interval training (HIIT) (Hawley & Gibala, 2012).

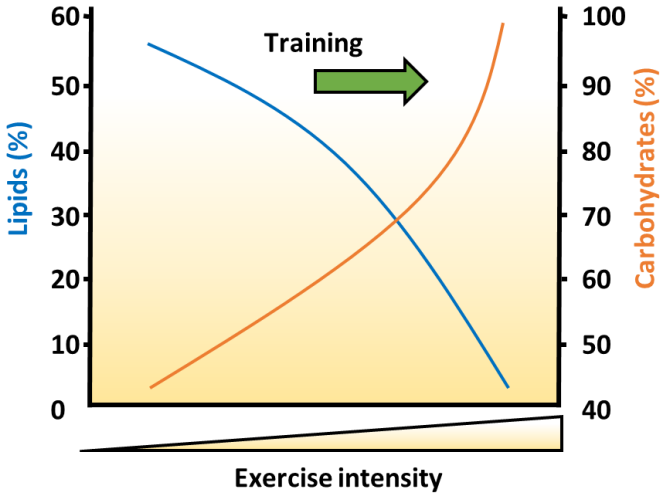

Figure 1: Exercise training and the concept of skeletal muscle metabolic flexibility. While exercise intensity increases, so does the relative contribution of carbohydrates for energy production. Exercise training allows a more efficient use of lipids and the sparing of glycogen stores in liver and muscle (adapted from Brooks and Mercier, 1994).

1.1.2.2 Weight-loss surgery

In extremely obese individuals (BMI ≥40 kg/m^2), lifestyle intervention can be insufficient to decrease weight and improve whole-body homeostasis. Weight-loss surgery, or bariatric surgery, is considered to be the most efficient strategy to treat extreme obesity, inducing major and durable weight loss (Carlsson *et al.*, 2012; Madsbad *et al.*, 2014), as well as decreasing mortality and morbidity (Adams *et al.*, 2007; Plecka Ostlund *et al.*, 2011). Yearly, there are more than 350,000 bariatric surgery interventions worldwide (Buchwald & Oien, 2009). Patients eligible for bariatric surgery must have a BMI ≥40 kg/m2 or ≥35 kg/m^2 in combination to a comorbidity, such as T2D.

Laparoscopic Roux-en-Y gastric bypass surgery (RYGB) is a malabsorptive surgical procedure that creates a pouch of 30 mL at the distal end of the stomach, causing the nutrients to bypass the rest of the stomach and the

upper part of the small intestine. RYGB patients experience higher satiety and decreased hunger, leading to a progressive average loss of 62% of the excess weight and maximum weight loss is generally achieved 1.5-2.0 years after the intervention (Buchwald *et al.*, 2004). Early metabolic changes occurring in patients after RYGB include improved glycemic control and insulin sensitivity. The changes in whole-body glucose homeostasis often occur before surgery-induced weight loss. Importantly, 70% to 80% of patients having T2D as a comorbidity get off from their anti-diabetic medication and undergo remission (Buchwald *et al.*, 2004; Sjostrom *et al.*, 2004).

RYGB is an invasive surgical procedure and is not without complications or consequences. Depending on the type of procedure, surgical complications can occur and require a second operation (Buchwald *et al.*, 2014). Malabsorption of micronutrients (vitamins, iron, zinc) can happen after RYGB (Tack & Deloose, 2014). Moreover, RYGB does not "protect" from the reward aspect of food or reverse hedonic hunger or food cravings (Delin *et al.*, 1997). Patients can also experience early or late dumping-like symptoms (sweating, tachycardia, nausea, and diarrhea) following meal ingestion (Tack & Deloose, 2014). Finally, re-gaining weight is still possible, although the prevalence and amount of weight depends on the surgical procedure (Sjostrom *et al.*, 2004).

To summarize, skeletal muscle plasticity allows functional and molecular adaptations following various exercise stimuli and/or dramatic weight loss interventions. The discovery of new targets, mechanisms or genetic variations associated with exercise response and subsequent improvements in metabolic status will facilitate the development of potential new avenues to treat and manage diseases (Fig. 2).

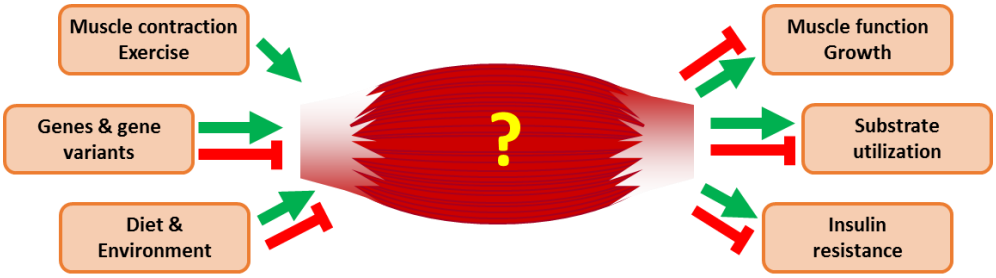

Figure 2: Unraveling mechanisms of skeletal muscle plasticity in response to various physiological and genetic stress factors. Green and red arrows indicate a potential positive or negative impact, respectively.

1.2 SKELETAL MUSCLE PHYSIOLOGY AND METABOLIC PROPERTIES

1.2.1 Skeletal muscle and exercise

Skeletal muscle represents more than 40% of total body mass and accounts for 30% of the basal metabolic rate (Zurlo *et al.*, 1990). This tissue is the main site of insulin-stimulated glucose uptake and consumes 80% of circulating glucose under resting conditions, thus playing a central role in whole-body glucose and energy homeostasis (DeFronzo *et al.*, 1981). Exercise plays a key role in the prevention and treatment of obesity and T2D. During physical exercise, whole-body metabolic rate can increase by up to 20-fold and ATP turnover, by 100-fold (Gaitanos *et al.*, 1993). Both acute exercise and repeated bouts of exercise (i.e. training) have a positive impact on whole-body energy metabolism and insulin sensitivity. Following an acute bout of exercise, improvements in whole-body insulin sensitivity and glucose tolerance persist for 48 hours (Mikines *et al.*, 1988), highlighting the potency of physical activity as a remedy for metabolic disease.

During exercise, skeletal muscle increases ATP turnover to meet the high-energy demand placed upon the organism (Gallagher *et al.*, 1998). Muscle contraction stimulates glucose uptake through an insulin-independent pathway, enhancing glucose disposal despite insulin resistance or T2D (Wallberg-Henriksson & Holloszy, 1984, 1985). Following metabolic or mechanical stimuli,

skeletal muscle exhibits extensive plasticity to maintain energy balance under diverse physiological conditions, ranging from starvation to nutrient excess. Physical activity, or lack thereof, profoundly impacts skeletal muscle function in a "use it or lose it" manner, altering molecular pathways that control fuel utilization, muscle growth, as well as oxidative properties.

1.2.2 Insulin signaling

1.2.2.1 Insulin-mediated glucose uptake

Insulin stimulates glucose entry into skeletal muscle for storage or utilization as an energy substrate. Insulin binding to the insulin receptor on the cell membrane results into auto-phosphorylation of the receptor and activation of its tyrosine kinase activity (Hubbard *et al.*, 1994). The activated insulin receptor subsequently phosphorylates insulin receptor substrates (IRS) (White *et al.*, 1985). This activates the phosphoinositide 3-kinase (PI3K) signaling cascade (Bellacosa *et al.*, 1998), leading to phosphorylation and activation of Akt and downstream effectors, including Akt-substrate of 160 kDa (AS160). AS160 activation ultimately results in the translocation of glucose transporter GLUT4 from the intracellular pool to the plasma membrane and allows glucose to enter the cell (Sano *et al.*, 2003). Akt phosphorylation and activation also stimulates glycogen, lipid and protein synthesis (Fig. 3).

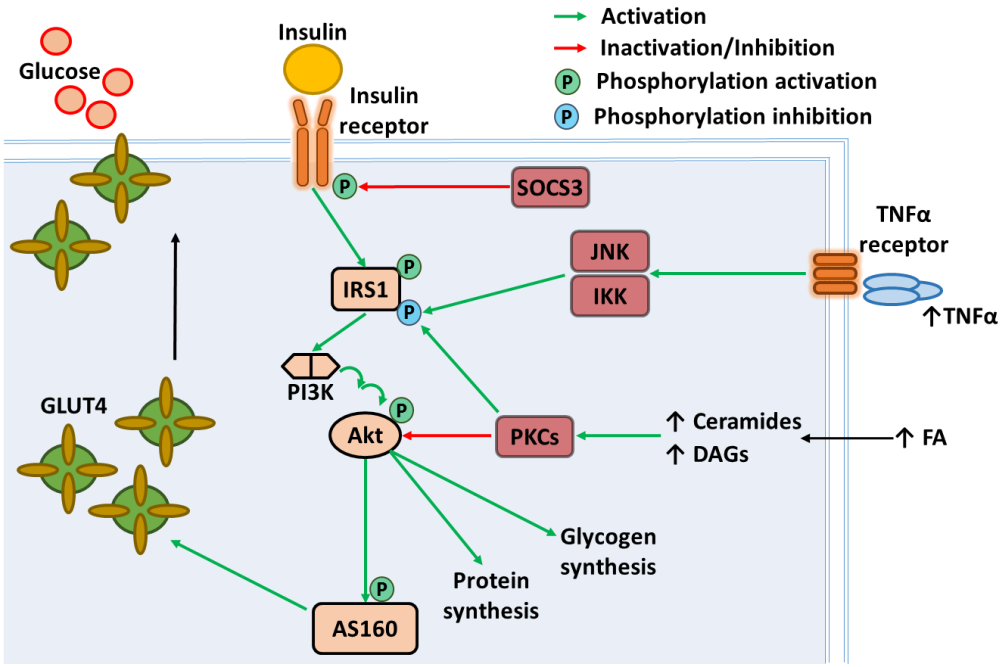

Figure 3: Insulin signaling and insulin resistance in skeletal muscle. Increased circulatory levels of fatty acids (FA) can lead to increased intracellular levels of ceramides and diacylglycerols (DAGs), which together with elevated levels of stress signaling kinases JNK and IKK and SOCS3, negatively regulate the insulin signaling cascade.

1.2.2.2 Skeletal muscle insulin resistance

Obese individuals have an increased reliance on carbohydrates vs. lipids compared to healthy lean individuals (Tremblay *et al.*, 1989) and an incapacity to increase the contribution of lipids as a substrate for energy production during physical activity (Battaglia *et al.*, 2012). Insulin resistance is a characteristic feature of the metabolic syndrome and precedes T2D. Insulin resistance arises from defects in insulin-stimulated glucose transport and insulin signaling, due in part from altered lipid metabolism and inflammatory responses (Fig. 3). High levels of circulating fatty acids and accumulation of intramuscular lipid intermediates are involved in the development of insulin resistance (Krssak *et al.*, 1999). Notably, the accumulation of diacylglycerol in skeletal muscle impairs intracellular signaling by activating members of the protein kinase C (PKC) family of signaling intermediates (Itani *et al.*, 2002; Szendroedi *et al.*, 2014), while ceramides negatively impact Akt signaling (Stratford *et al.*, 2004; Holland *et al.*,

2011). Chronic low-grade inflammation also impairs insulin signaling in skeletal muscle. Increased circulating levels of TNFα activates intracellular stress kinases IκB kinase (IKK) and c-Jun terminal kinase (JNK), inducing inhibitory serine phosphorylation of IRS (Aguirre *et al.*, 2000; Werner *et al.*, 2004). Finally, elevated levels of suppressor of cytokine signaling 3 (SOCS3) are reported in skeletal muscle from T2D patients (Rieusset *et al.*, 2004; Mashili *et al.*, 2013). SOCS3 negatively regulates insulin signaling by inhibiting tyrosine kinase activity of the insulin receptor (Emanuelli *et al.*, 2000).

1.2.2.3 Contraction-mediated glucose uptake

Through an insulin-independent mechanism (Nesher *et al.*, 1985; Lee *et al.*, 1995), skeletal muscle contraction results into the translocation of GLUT4 to the plasma membrane and the subsequent entry of glucose into the muscle cell (Lund *et al.*, 1995). Muscle contraction stimulates calcium release from the sarcoplasmic reticulum leading to an increased AMP:ATP ratio into the cell. This increase in the AMP:ATP ratio activates an energy sensor of the cell, namely AMP-activated protein kinase (AMPK), which in turn phosphorylates AS160 (Treebak *et al.*, 2006). Both insulin- and contraction-mediated glucose uptake signaling are summarized in Fig. 4.

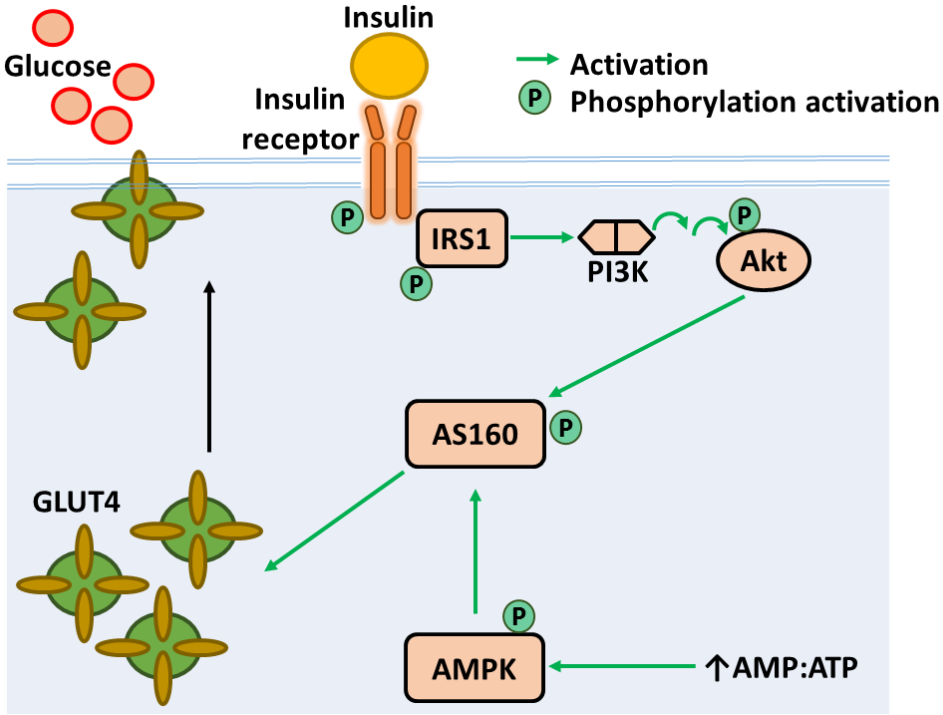

Figure 4: Insulin and contraction-mediated glucose uptake. Insulin binds to the insulin receptor and triggers the insulin signaling cascade, ultimately leading to the translocation of the glucose transporter (GLUT4) from the intracellular pool to the plasma membrane and to glucose uptake into the cell. AMPK activation also leads to GLUT4 translocation and glucose uptake.

1.2.3 The sarcomere

Skeletal and cardiac muscle are sometimes referred as "striated muscle" because of their striated aspect resulting from the highly ordered longitudinal alignment of sarcomeres, the contractile and functional units of muscle. The borders of the sarcomere are defined by the Z-line, while the M-line stands in the middle. The sarcomere is mainly composed of contractile proteins myosin (thick filament) and actin (thin filament) and muscle contraction occurs through actin-myosin cross-bridge cycling, according to the sliding filament theory (Huxley & Niedergerke, 1954; Huxley & Hanson, 1954). Actin filaments are cross-linked together by alpha-actinin (α-actinin) at the Z-line (Masaki *et al.*, 1967). Giant

protein titin spans from the Z-line to the M-line and stabilizes the actin-myosin filament (Wang *et al.*, 1979; Labeit & Kolmerer, 1995). Nebulin is another giant protein that forms a helix with the actin protein and serves as molecular ruler (Labeit *et al.*, 1991). Several other structural sarcomeric proteins including capping proteins, calsarcins, myotilin, myopalladin, and PDZ and LIM domain proteins are located at the Z-line and interact with, among others, α-actinin. A simplified version of the molecular architecture of the sarcomere is presented (Fig. 5).

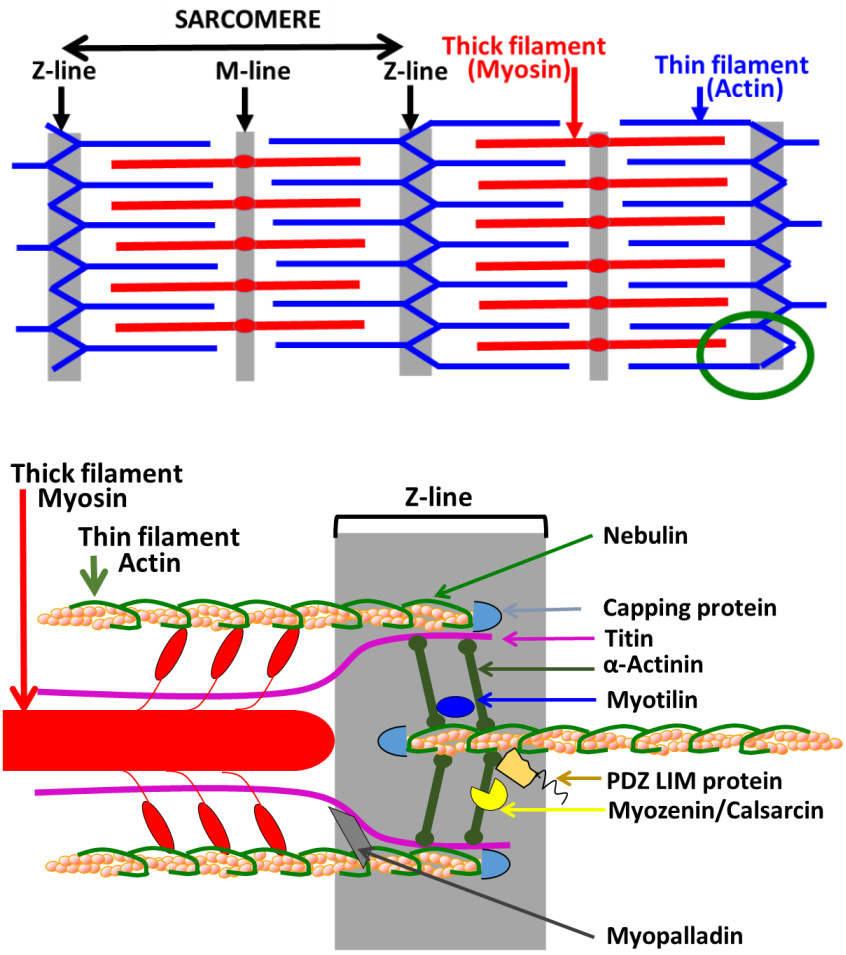

Figure 5: Schematic representation of the sarcomere and Z-line proteins.

1.2.4 Skeletal muscle fiber type

The capacity of skeletal muscle to adapt to stressors is largely defined by the structural and functional characteristics of the muscle fibers. Several different muscle fibers exist and their classification is based on sarcomeric myosin heavy chain (MyHC) isoform composition, speed of contraction and resistance to fatigue properties (Schiaffino & Reggiani, 2011). Different fiber types can also co-exist heterogeneously in the same muscle (Schiaffino *et al.*, 1970). Skeletal muscle fiber type is divided between type 1, slow-twitch, oxidative fibers, and type 2, fast-twitch, glycolytic fibers (Needham, 1926; Buller *et al.*, 1960). Type 2 fibers are subdivided in three distinct types, fast-twitch oxidative glycolytic type 2A, 2X and 2B (Larsson *et al.*, 1991; DeNardi *et al.*, 1993). The power generated by muscle contraction is directly related to the ATP hydrolysis rate of myosin (Barany, 1967). Type 1 fibers have a low rate of ATP utilization and a slow contracting speed and power, but are fatigue resistant. They are also rich in mitochondria and myoglobin (Schiaffino *et al.*, 1970). Type 2 fibers can generate powerful and rapid contractions, but are more fatigue-prone and consume a higher rate of ATP. They contain less mitochondria than type 1 fibers and have low to intermediate levels of myoglobin (Schiaffino *et al.*, 1970). Among type 2 fibers, type 2A is the most fatigue resistant and type 2B is the most fatigue prone, but also the "most powerful" (2B > 2X > 2A) (Larsson *et al.*, 1991). The Z-line is thicker in type 2 fibers than in type 1 fibers. Variability in fiber type distribution exists between rodents and humans. While mice have a higher proportion of type 2, fast-twitch, muscle fibers, humans display a higher proportion of slow-twitch muscle fibers (Pellegrino *et al.*, 2003).

Metabolic properties are tightly linked to the structural architecture and composition, which varies according to skeletal muscle fiber type. Type 1 oxidative fibers contain a higher amount of GLUT4 and have a high rate of glucose uptake (Goodyear *et al.*, 1991). All muscle fibers can store and utilize glycogen and lipids, with type 2 fibers containing more glycogen than type 1 and type 1 fibers being glycogen-depleted before type 2 in response to exercise (Vollestad *et al.*, 1984; Greenhaff *et al.*, 1993). Transport, storage and utilization of fatty acids is larger in type 1 fibers than in type 2 fibers (Chabowski *et al.*, 2006). Given that

muscle fiber type influences glucose and lipid metabolism, differences in fiber type composition or changes in metabolic properties resulting from lifestyle alterations or physical inactivity could be involved to the development of insulin resistance and metabolic diseases.

1.3 REGULATION OF EXERCISE ADAPTATIONS

Repeated bouts of exercise or muscle contraction triggers alterations in mRNA expression, protein abundance and enzyme activity, resulting into chronic functional and physiological adaptations of skeletal muscle to support greater energy demands (Egan & Zierath, 2013). To regulate exercise adaptations, different signaling pathways are at work and the type of exercise performed will modulate the molecular changes leading to a particular physiological response.

1.3.1 Muscle contraction and calcium signaling

The induction of an action potential by the motoneuron induces calcium ion (Ca^{2+}) release from the sarcoplasmic reticulum. Ca^{2+} subsequently binds to troponin, which exposes the actin-binding site for myosin. Myosin attaches to actin to form actomyosin cross-bridges and muscle contraction occurs (Podolsky & Schoenberg, 1983). In addition to contraction, calcium is also involved in the adaptive response of skeletal muscle to exercise. Intermediates of calcium signaling include the protein phosphatase calcineurin. Calcineurin regulates the transcriptional activity of calcineurin-dependent nuclear factor of activated T-cells (NFAT) and modulates the expression of genes involved in the determination of the fast/slow phenotype of skeletal muscle fibers (Im & Rao, 2004; McCullagh *et al.*, 2004).

1.3.2 The cellular energy sensor AMPK

The serine/threonine protein kinase AMPK monitors the energy state of the cell by sensing both AMP:ATP and ADP:ATP ratios (Hardie, 2014). High energy demand increases the rate of ATP hydrolysis in the cell, causing AMP and ADP levels to rise. When an organism is under conditions of metabolic stress that decrease ATP levels, such as starvation and endurance exercise, AMPK acts as

molecular switch to restore ATP levels and energy homeostasis. Both adenine nucleotides bind to the γ regulatory subunit of AMPK, triggering phosphorylation of the Thr172 residue of the catalytic α subunit, and increasing kinase activity by more than 100-fold (Hawley *et al.*, 1996). Moreover, the allosteric activation of AMPK by binding of AMP to the γ regulatory subunit inhibits dephosphorylation by protein phosphatases by altering the conformation of the heterotrimer (Davies *et al.*, 1995; Xiao *et al.*, 2011). Upon activation, AMPK activates energy-producing pathways, such as glucose transport and lipid oxidation while simultaneously halting energy-consuming processes such as protein and lipid synthesis. Because of its role in fuel source switching, AMPK constitutes an attractive target in the context of metabolic disease.

AMPK consists of a catalytic α subunit, a regulatory β subunit and a regulatory γ subunit. The combination of the different isoforms (α1/α2, β1/β2, γ1/γ2/γ3) of the subunits leads to a possibility of 12 different heterotrimers, highlighting the possibility that AMPK isoforms have different functional roles. Indeed, tissue-specific heterotrimeric combinations exist and impact metabolism and the response to exercise (Klein *et al.*, 2007; Kjobsted *et al.*, 2014). In skeletal muscle, the α2β2γ3 is the predominant AMPK complex. The γ3 isoform, encoded by the PRKAG3 gene, is the most widely expressed isoform of the γ subunit in human skeletal muscle and its expression is highly specific to glycolytic white skeletal muscle (Mahlapuu *et al.*, 2004). The discovery of the R200Q non-conservative substitution in the PRKAG3 gene in Hampshire pigs prompted attention for a role of the muscle-specific γ3 isoform in energy metabolism (Milan *et al.*, 2000). Skeletal muscle from pigs carrying the mutation has a low ultimate pH (measured 24 hours after slaughter), reduced water holding capacity and increased glycogen content (Milan *et al.*, 2000). The phenotype resulting from the mutation has a negative impact on meat industry economics and pig breeding industry. This mutation can also be found in humans (Costford *et al.*, 2007). In mice, the R225Q single-nucleotide polymorphism in the Prkag3 gene mimics the PRKAG3 R200Q mutation in pigs and also results in an altered glycogen phenotype (Barnes *et al.*, 2004). The *in vivo* effects of the R225Q mutation were extensively characterized using Tg-Prkag^{wt}, Tg-Prkag3^{225Q} and Prkag3$^{-/-}$ mice

models (Barnes *et al.*, 2004; Barnes *et al.*, 2005a; Barnes *et al.*, 2005b; Garcia-Roves *et al.*, 2008).

1.3.3 Skeletal muscle hypertrophy

Adaptations to resistance-based exercise ultimately lead to an increase in protein synthesis, muscle hypertrophy (the enlargement of pre-existing muscle fibers) and the development of a greater force production (Egan & Zierath, 2013). The IGF1/PI3K/Akt pathway mediates signal transduction leading to cell growth and skeletal muscle hypertrophy. Insulin and insulin-like growth factor 1 (IGF1) bind to the IGF1 and the insulin receptors, resulting in the phosphorylation of IRS1 (White *et al.*, 1985; Izumi *et al.*, 1987; Hubbard *et al.*, 1994) and the stimulation of the PI3K/Akt pathway. When activated, Akt directly phosphorylates and inhibits tuberous sclerosis complex 2 (TSC2), which in turn activates the serine threonine protein kinase mammalian target of rapamycin complex 1 (mTORC1) (Inoki *et al.*, 2002). mTORC1 subsequently phosphorylates of p70S6k and downstream effectors of p70S6k include ribosomal protein S6 (RPS6) and eukaryotic initiation factor 4E-binding protein 1 (4E-BP1), whose phosphorylation by p70S6k results in activation and inhibition, respectively, leading to ribosomal biogenesis and protein translation/elongation (Bodine *et al.*, 2001). mTORC1 is a complex including the serine threonine protein kinase mTOR, regulatory-associated protein of mTOR (Raptor), and proline-rich Akt substrate of 40 kDa (PRAS40). This complex integrates various molecular signals and consequently regulates protein synthesis and degradation (Zhang *et al.*, 2014). In addition to be a member of mTORC1, PRAS40 is a substrate for Akt and could play a role in improved insulin signaling and sensitivity in skeletal muscle (Wiza *et al.*, 2014).

Skeletal muscle growth and protein synthesis depend on the fine-tuning between the energy sensors AMPK and mTORC1 since they are likely to have antagonistic effects on the control of metabolism and on the size of the muscle cell (Mounier *et al.*, 2011). Impaired signaling of mTORC1 and its downstream effectors (such as p70S6k) results in defective muscle cell growth, which correlates with increased AMPK activation (Mounier *et al.*, 2011). AMPK

activation inhibits protein synthesis and impairs Akt/mTOR signaling (Bolster *et al.*, 2002), notably via TSC2 or Raptor (Inoki *et al.*, 2003; Gwinn *et al.*, 2008). While the role of mTORC1 is to promote skeletal muscle hypertrophy, the role of AMPK is to limit muscle growth or promote skeletal muscle atrophy (Fig. 6).

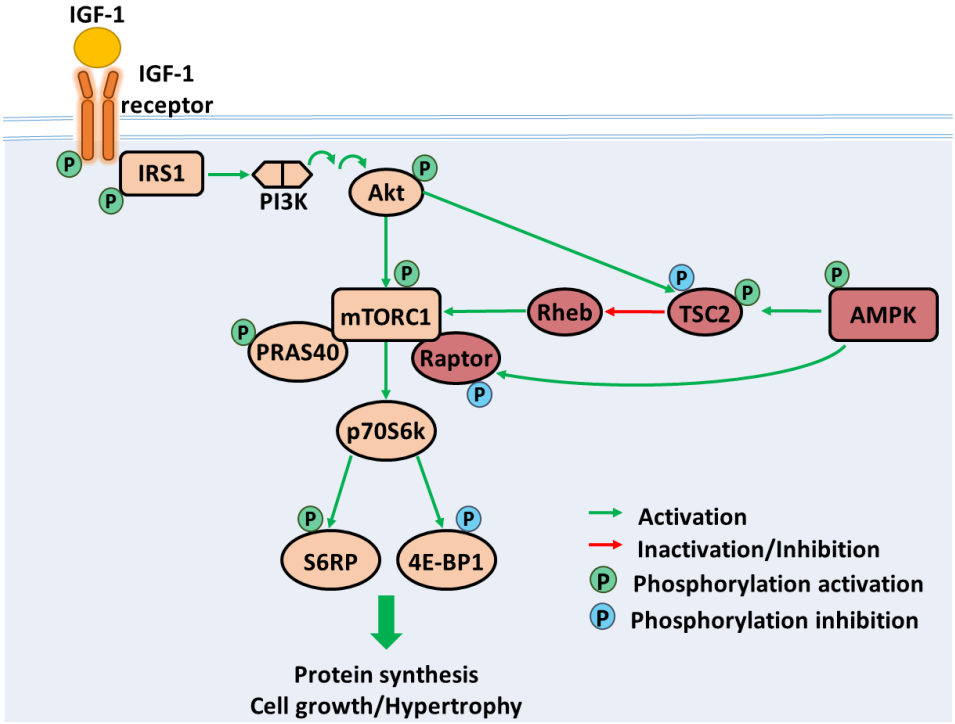

Figure 6: Crosstalk between mTORC1 and AMPK signaling. IGF1 binds to its membrane receptor and triggers the IGF1 signaling cascade, ultimately leading to phosphorylation of downstream effectors of mTORC1 resulting into protein synthesis and muscle hypertrophy. AMPK represses mTORC1 activity by phosphorylating TSC2 and Raptor.

Skeletal muscle growth and hypertrophy is also associated with changes in other hypertrophic/atrophic markers. For instance, the activation of protein synthesis by the IGF1/PI3K/Akt signaling cascade is accompanied by changes in atrophic markers E3 ubiquitin ligases, including Mafbx and MuRF1 (Latres *et al.*, 2005). Myostatin is also a negative regulator of muscle mass (McPherron *et al.*, 1997) and represses Akt signaling (Sartori *et al.*, 2009). Gene expression of a splice variant originating from the alternative promoter of PGC1α, named PGC1-

α isoform 4 (PGC1α4) (Ruas *et al.*, 2012) is also up-regulated in resistance exercise in humans and prevents skeletal muscle atrophy induced by cancer-cachexia. However, the precise role of PGC1α4 in the regulation of skeletal muscle hypertrophy is still controversial (Perez-Schindler *et al.*, 2013; Lundberg *et al.*, 2014).

AMPK and mTOR regulate autophagy, a self-digestive, tightly-regulated, cellular process where cytoplasmic components are degraded to generate nutrients and energy for the cell, by exerting opposite effects. Nutrient deprivation, acute exercise and subsequently AMPK activation, promotes autophagy by activating transcription factor forkhead box O3 (FOXO3) and by repressing mTOR (Kim *et al.*, 2011; Sanchez *et al.*, 2012). Autophagy is required for exercise training-induced adaptations in skeletal muscle (He *et al.*, 2012). Thus, another mechanism by which AMPK may possibly control muscle mass is by modifying autophagy.

1.3.4 Gene variants as determinants of exercise performance

Both genetic and environmental factors contribute to the development of metabolic disease. In the same way that gene variants impact T2D (Bonnefond *et al.*, 2010; Dimas *et al.*, 2014), the response to exercise can be inherited (Bouchard *et al.*, 1998; De Moor *et al.*, 2007). Heritability can account for approximately 50% of the variation in aerobic capacity, as evaluated by VO_2max in untrained individuals or in response to exercise training (Bouchard *et al.*, 1998; Bouchard *et al.*, 1999). Several genetic traits are also associated to endurance or sprint- and power-based exercise performance. Those include the angiotensin-converting enzyme insertion/deletion (ACE I/D), where the I allele is associated with endurance performance, while the D allele associates with sprint and power performance (Rigat *et al.*, 1990; Danser *et al.*, 1995). A polymorphism in the ACSL1 gene (rs6552828), an enzyme involved in cellular lipid handling, accounts for 3.5% of VO_2max trainability (Bouchard *et al.*, 2011). However, the gene variant most consistently associated to athletic performance in humans is the ACTN3 R577X polymorphism (Eynon *et al.*, 2013).

1.3.5 The ACTN3 R577X polymorphism

The α-actinin protein was first identified in 1965 (Ebashi & Ebashi, 1965) and was reported to be very similar to actin, citing a possible role in skeletal muscle contraction. Following early experiments revealing that α-actinin was necessary for maximal binding of actin and myosin (Ebashi & Ebashi, 1965), α-actinin was recognized as an actin crosslinking Z-line protein (Masaki *et al.*, 1967). Later, its complete amino acid sequence was published (Arimura *et al.*, 1988). Different skeletal muscle-specific isoforms α-actinin 2 and 3 (encoded by genes ACTN2 and ACTN3) were then discovered (Beggs *et al.*, 1992) and in 1996, the α-actinin 3 protein was reported to be specific to glycolytic skeletal muscle (North & Beggs, 1996). Very recently, the crystal structure of human skeletal muscle α-actinin was published, providing new insight into the molecular architecture of the Z-line (Ribeiro Ede *et al.*, 2014).

The ACTN3 R577X polymorphism (rs1815739) is a common nonsense polymorphism due to the transition of C for a T in the nucleotide sequence, substituting an arginine (R) for a stop codon (X) at amino acid 577 (North *et al.*, 1999). Consequently, carriers of the ACTN3 577XX genotype do not express α-actinin protein. Although the SNP was identified in the context of work focusing on neuromuscular diseases, no disease phenotype is known to arise from the absence of α-actinin 3 in skeletal muscle. Following the identification of the SNP and because of the fiber type-specificity of ACTN3 expression, genotyping of various athlete cohorts established an association between the R577X polymorphism and muscle performance. The 577RR genotype is underrepresented in athletes specializing in power and strength-focused activities, such as sprint and heavy weight-lifting, when compared to endurance athletes or to healthy control individuals (Yang *et al.*, 2003; Niemi & Majamaa, 2005; Druzhevskaya *et al.*, 2008; Papadimitriou *et al.*, 2008; Roth *et al.*, 2008). At the other end of the exercise continuum, elite endurance athletes display a higher prevalence of the 577XX genotype compared to healthy controls (Yang *et al.*, 2003; Niemi & Majamaa, 2005; Eynon *et al.*, 2009; Shang *et al.*, 2010).

The prevalence and distribution of the ACTN3 R577X polymorphism among the athlete population highlighted a potential role for α-actinin 3 in glucose or lipid metabolism in skeletal muscle (Berman & North, 2010). However, a clear biological and molecular mechanism linking the presence or absence of α-actinin 3 to skeletal muscle performance remains to be established. The generation of the ACTN3$^{-/-}$ mouse model offers insight into the mechanism by which α-actinin 3 impacts muscle performance (MacArthur *et al.*, 2007; MacArthur *et al.*, 2008; Quinlan *et al.*, 2010; Seto *et al.*, 2011; Seto *et al.*, 2013). ACTN3$^{-/-}$ mice have lower body weight and lean mass than wild-type counterparts, which could be partly explained by a smaller cross-sectional fiber surface area of glycolytic 2X muscle fibers. Muscle fiber type distribution is unaltered between ACTN3$^{-/-}$ and wild-type. Furthermore, ACTN3$^{-/-}$ mice have enhanced endurance performance (run to exhaustion) and decreased grip strength compared to wild-type littermates. Skeletal muscle metabolic properties of ACTN3$^{-/-}$ mice shift towards an oxidative phenotype, together with increased glycogen content and glycogen phosphorylase activity. Finally, ACTN3$^{-/-}$ mice also show higher susceptibility to muscle damage when subjected to extreme eccentric contractile activity. α-Actinin 2 protein abundance is increased in skeletal muscle of ACTN3$^{-/-}$ mice, presumably as a compensatory response for the lack of α-actinin 3. Recently, ACTN3 was shown to reprogram skeletal muscle in response to training by promoting a shift toward an oxidative fiber phenotype via calcineurin signaling (Seto *et al.*, 2013). In humans, a role for α-actinin 3 has been investigated in the context of McArdle's disease (Lucia *et al.*, 2007), spinal cord injury (Broos *et al.*, 2012), aging (Zempo *et al.*, 2011), and muscle immobilization (Garton *et al.*, 2014). However, the relationship between the presence or absence of α-actinin 3 and metabolic diseases remains unexplored.

2 AIMS

Detailed understanding of the molecular mechanisms regulating skeletal muscle response to either metabolic or hypertrophic stimuli is vital for the development and improvement of current existing therapeutic interventions and for the discovery of potential new targets to treat metabolic disease.

Therefore, the overarching aim of this thesis is to unravel mechanisms associated with the development of insulin resistance in metabolic disease by characterizing pathways regulating metabolism and growth in skeletal muscle.

The specific aims of this thesis include:

- To evaluate the myogenic and metabolic profile from primary skeletal muscle cells derived from severely obese people before and after gastric bypass surgery.

- To examine the prevalence of the ACTN3 R577X polymorphism in a cohort of people with NGT, IGT, or T2D and to determine the impact of this polymorphism on glucose metabolism, mitochondrial complex enzymes, and the skeletal muscle contractile network.

- To determine the contribution of the γ3 subunit of AMPK on the hypertrophic response of skeletal muscle to functional overload.

3 METHODS

3.1 STUDY PARTICIPANTS

In Study I, 8 obese non-diabetic subjects (1 male and 7 female), underwent laparoscopic RYGB surgery. A subset of the subjects have been included in a previous study (Barres *et al.*, 2013). The clinical characteristics of these participants are presented in Paper I, Table 1. For Study II, 177 male and female volunteers with NGT or T2D were included in the study. The initial analysis also included patients with IGT, leading to a total of 211 participants. The entire cohort was also studied previously (Fritz *et al.*, 2011; Fritz *et al.*, 2013) and the clinical parameters describing the NGT and T2D participants are presented in Paper II, Table 1. The clinical characteristics of the IGT subjects are included in Table 4. All participants provided written informed consent and all protocols were approved by the Ethics Committee of Karolinska Institutet.

3.1.1 Anthropometric and metabolic measurements

Upon enrolment, participants to **Study II** underwent a complete medical examination and anthropometric and metabolic characteristics were measured. Participants were classified as NGT, IGT or T2D following an OGTT performed as described (Fritz *et al.*, 2011; Fritz *et al.*, 2013). Inclusion criteria for all groups were an age range of 45–69 years old and a BMI > 25 kg/m^2. T2D patients had HbA_{1c} levels ranging from 7.4% to 9.8%. Exclusion criteria were physical impairments, symptomatic angina pectoris, atrial fibrillation measured by ECG, systolic or diastolic blood pressure >160 and >100 mmHg, respectively, or insulin treatment. Cardiorespiratory fitness was assessed by measuring oxygen uptake using a ramp test on a mechanically braked ergometer as described previously (Fritz *et al.*, 2013).

3.1.2 Skeletal muscle biopsies

For **Studies I and II**, skeletal muscle biopsies were obtained from the participants. Biopsies (20–100 mg) were obtained from the *vastus lateralis* portion of the *quadriceps femoris* muscle using a Weil-Blakesley conchotome

(Dietrichson *et al.*, 1987) under either general (**Paper I**) or local anesthesia (lidocaine hydrochloride 5 mg/mL; **Paper II**) after an overnight fast. Biopsies were washed and either put in PBS at 4°C (**Paper I**) or immediately snap-frozen in liquid nitrogen (**Paper II**).

3.2 ANIMALS AND SURGICAL PROCEDURES

3.2.1 Genetically modified mouse models

The Tg-Prkag3^{225Q} and Prkag3$^{-/-}$ mice used for **Study III** were previously generated and extensively characterized (Barnes *et al.*, 2004; Barnes *et al.*, 2005a; Barnes *et al.*, 2005b). Mice had free access to standard rodent chow (4% fat, 16.5% protein, 58% carbohydrates, 3.0 kcal/g; Lantmännen, Stockholm, Sweden) and water. Animals were housed with same-sex littermates and kept on a 12 hr light-dark cycle at constant temperature and humidity. All procedures were approved by the Stockholm North Ethical Committee and conducted in agreement with the regulations for protection of laboratory animals.

3.2.2 Functional overload using the synergistic ablation model

Tg-Prkag3^{225Q} and Prkag3$^{-/-}$ male mice and wild-type littermates underwent functional overload of the plantaris muscle at 13 to 15 weeks of age. Functional overload was accomplished by bilateral surgical removal of the soleus and gastrocnemius muscles (Baldwin *et al.*, 1981; Bodine & Baar, 2012). Mice were first anesthetized with isoflurane. An incision was made on the side of the leg from the ankle to the knee. The soleus and gastrocnemius muscles were excised and the skin of the leg was sutured back together (Fig. 7). In the control condition, mice were sham-operated: the plantaris, soleus, and gastrocnemius muscles were gently separated from each other with blunt ends forceps. During and following the surgical procedure, mice were given the analgesic buprenorphine (Temgesic; 0.05-0.1 mg/kg, RB Pharmaceuticals Limited, Slough, UK) by subcutaneous injection. After 14 days, fed mice were anesthetized with Avertin (0.02 mL/g; 2.5% solution of 99% 2,2,2-tribromo ethanol and tertiary amyl alcohol) by intra-peritoneal injection, plantaris muscles were removed, weighed, snap-frozen in liquid nitrogen, and stored at -80°C until further processing. To measure lean and

fat mass, mice underwent magnetic resonance imaging (EchoMRI-100; EchoMRI, Houston, USA) prior to the functional overload procedure and collection of the plantaris muscle.

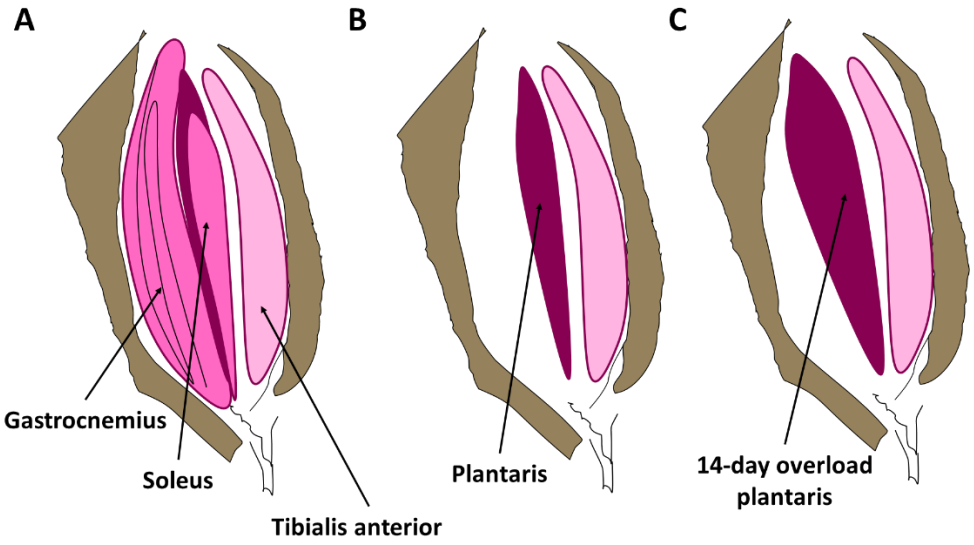

Figure 7: Synergistic ablation model. A) View from the *tibialis anterior*, soleus and gastrocnemius muscles following lateral incision of the mouse hindlimb B) Excision of soleus and gastrocnemius muscles C) Plantaris muscle undergoes hypertrophy.

3.3 CELL CULTURE

3.3.1 Growth and differentiation of primary human skeletal muscle cells

For **Study I**, primary human myoblasts were isolated from biopsies taken before and six months after gastric bypass surgery from *vastus lateralis* muscle of 8 subjects and propagated *in vitro* (Al-Khalili *et al.*, 2003). For **Study II**, commercially available primary myoblasts were purchased from Lonza (#CC-2561, Copenhagen, Denmark). Myoblasts were grown in Dulbecco's Modified Eagle Medium (DMEM) Nutrient Mixture F12 (Gibco, Life Technologies, Stockholm, Sweden) supplemented with 20% fetal bovine serum (FBS; Gibco), 1% penicillin/streptomycin (Gibco) and 1% Fungizone® (Gibco). When reaching 80% confluence, cells were passaged using trypsin digestion (TrypLE™ Express Enzyme; Gibco). Cells were plated in 6-well plates for individual experiments. At

90% confluence, myoblasts were differentiated into myotubes by the addition of a low-serum media (DMEM + glutamax (1 g/L glucose; Gibco) supplemented with 2% (2 first days of differentiation) to 4% FBS (after day 2 post-differentiation), 1% penicillin/streptomycin and 1% Fungizone®. Metabolic assays were performed on day 5 post-differentiation. Cell cultures were maintained at 37°C under 7.5% CO_2.

3.3.2 Metabolic assays – Glucose incorporation into glycogen

Glucose conversion into glycogen was determined by incubating myotubes with [^{14}C]-labelled glucose, precipitation of newly synthetized glycogen and determination of radioactivity. Fully differentiated myotubes were serum-starved for 4 hours and subsequently incubated for 30 min in the presence or absence of 120 nM of insulin (Actrapid, Novo Nordisk, Copenhagen, Denmark). Insulin was diluted in DMEM and bovine serum albumin (Sigma-Aldrich, St. Louis, MO, USA). Myotubes were incubated with 50 ng/ml of recombinant IL8 (Sigma-Aldrich) for 2 hours prior to the insulin treatment as indicated in figure legends of **Paper I**. Radioactive-labelled glucose (D-[U-^{14}C]-glucose with 1 µCi/ml; Perkin-Elmer) was diluted into DMEM and 1 mL was added to the cells, which were incubated for 90 min. After incubation, cells were rapidly washed 3 times with ice-cold PBS and frozen at -20°C. Cells were thawed and lysed using 500 µL of 0.03% SDS per well. A volume of 350 µL of the cell lysate was transferred to 2 mL tubes to which 0.2 mg of glycogen carrier (Sigma-Aldrich) was added. Protein concentration was determined using a bicichoninic acid protein assay kit (Pierce, Rockford, IL, USA). Samples were boiled for 60 min and 1.5 mL of 99% ethanol was added to the tubes which were stored at -20°C overnight for glycogen precipitation. Samples were then subjected to centrifugation (10,000 rpm for 15 min) at room temperature and ethanol was removed. Samples were washed twice with 1.2 mL of 70 % ice-cold ethanol. After the last wash, samples were left to dry at room temperature and glycogen was dissolved in 400 µL of water overnight. A 200 µL aliquot of the sample was added to a scintillation vial containing 2.8 mL of scintillation liquid (Ultima Flo™ M, Perkin-Elmer) and radioactivity was determined with a beta-counter (Wallac, Turku, Finland).

3.3.3 Metabolic assays – Palmitate oxidation

Utilization of the fatty-acid palmitate was measured *in vitro* by treating fully differentiated myotubes with [^{3}H]-labeled palmitate and measuring the [^{3}H]-labeled water, an end product of fatty-acid beta-oxidation. Myotubes were serum-starved for 2 hours and subsequently incubated for 6 hours in 1 mL of DMEM with or without 20 μM or 500 μM palmitic acid (Sigma-Aldrich) supplemented with 0.5 μCi [^{3}H] radioactivity-labeled [9-10-^{3}H(N)] palmitic acid (Perkin-Elmer). Palmitic acid was supplemented with 50 ng/ml of recombinant IL8 (Sigma-Aldrich) as indicated in figure legends of **Paper I**. Cell media was then collected and cells were quickly washed 3 times in ice-cold PBS. To absorb the non-metabolized palmitate, 0.2 ml of cell media was added to 0.8 ml of charcoal slurry (0.1 g charcoal powder (Sigma-Aldrich) in 1 ml of 0.02 M Tris-HCl buffer, pH of 7.5) and shaken intermittently for 30 min. Samples were then subjected to centrifugation at 13,000 rpm for 15 min. Then 0.2 ml of supernatant with [^{3}H]-labeled water was pipetted into scintillation vials containing 2.8 ml of scintillation liquid and radioactivity was measured with a beta-counter (Wallac).

3.4 DNA EXTRACTION AND GENOTYPING

For **Paper II**, venous blood was collected from the participants after an overnight fast and stored in Vacutainer® tubes containing EDTA (BD, Stockholm, Sweden) and stored at -80°C for further analysis. Genomic DNA (gDNA) was extracted from 200 μL of whole blood using a commercial kit (Qiagen, Hilden, Germany) according to the manufacturer's instructions. Using 10 μg of input gDNA, genotyping for the ACTN3 R577X SNP was performed by PCR amplification (10 min at 95°C followed by 40 cycles of 15 seconds at 95°C for 1 min at 60°C) followed by allelic discrimination using fluorogenic probes (1 cycle of 1 min at 60°C; TaqMan® SNP Genotyping Assays, ID C_590093_1; Applied Biosystems, Foster City, CA, USA) using a thermal cycler (ABI 7000, Applied Biosystems). The same kit, reagents and protocol were used to genotype the human skeletal muscle cells.

3.5 RNA EXTRACTION AND GENE EXPRESSION MEASUREMENT

For **Studies II and III**, total RNA was extracted from 10 to 30 mg of human or mouse skeletal muscle using TRIzol® (Invitrogen, Carlsbad, CA, USA) according to the manufacturer's instructions. For **Study I**, RLT lysis buffer (Qiagen) was added directly to the plate well and cells were harvested into an RNase-free tube. RNA was then extracted using the RNeasy kit (Qiagen), according to the manufacturer's instructions. RNA concentration was measured using a spectrophotometer (NanoDrop, Thermo Scientific). cDNA was synthetized from 1-1.5 µg of RNA using either the High Capacity cDNA Reverse Transcription Kit from Applied Biosystems (**Studies I and III**) or the SuperScript First Strand Synthesis System from Invitrogen (**Study II**). Gene expression was measured by quantitative real-time PCR (RT-qPCR, StepOnePlusTM Real-Time PCR System; Applied Biosystems) using TaqMan® gene expression assays for **Studies I and II** and SYBR green primers **Study III**. Lists of primers can be found in Table 2 and 3. Reactions were performed in duplicate in a 96-well format and relative gene expression was calculated using the comparative CT method and normalized to a selected housekeeping gene for internal control (β2-microglobulin for **Study I**, beta-actin for **Study II**, and TATA box binding protein (Tbp) for **Study III**).

Table 2: List of TaqMan® assays used in Studies I and II.

Gene name	Gene ID	Cat. Number
Actin, alpha 1, skeletal muscle	ACTA1	Hs00559403_m1
Actinin, alpha 2	ACTN2	Hs01552477_m1
Actinin, alpha 3	ACTN3	Hs01100111_g1
beta-2-microglobulin	B2M	4326319E
Beta-actin	ACTB	4326315E
Capping protein (actin filament) muscle Z-line, alpha 1	CAPZA1	Hs04187789_g1
Capping protein (actin filament) muscle Z-line, alpha 2	CAPZA2	Hs00255135_m1
Capping protein (actin filament) muscle Z-line, beta	CAPZB	Hs01120796_m1
LIM domain binding 3	PDLIM6	Hs00951222_m1
Myotilin	MYOT	Hs00199016_m1
Myopalladin	MYOP	Hs00261515_m1
Myozenin 1	MYOZ1	Hs00222007_s1
Myozenin 2	MYOZ2	Hs00213216_m1
Myozenin 3	MYOZ3	Hs00911018_s1
Nebulin	NEB	Hs00189880_m1
PDZ and LIM domain 3	PDLIM3	Hs01062534_m1
Titin	TTN	Hs00399225_m1
Adiponectin	ADIPOQ	Hs00605917_m1
Carnitine palmitoyltransferase 1B (muscle)	CPT1B	Hs00189258_m1
Clock circadian regulator	CLOCK	Hs00231857_m1
Desmin	DES	Hs00157258_m1
Glycogen synthase 1 (muscle)	GYS1	Hs00157863_m1
Hexokinase 2	HK2	Hs01034050_g1
Myogenic differentiation 1	MYOD1	Hs00159528_m1
Myogenin	MYOG	Hs01072232_m1
Myostatin	MSTN	Hs00976237_m1
Paired-box 3	PAX3	Hs00240950_m1
Paired-box 7	PAX7	Hs00242962_m1
Peroxisome proliferator-activated receptor gamma, coactivator 1 alpha	PPARGC1A	Hs00173304_m1
Phosphoglycerate kinase 1	PGK1	Hs00943178_g1
Protein phosphatase, Mg2+/Mn2+ dependent, 1A	PPM1A	Hs01056778_g1
Pyruvate dehydrogenase kinase, isozyme 4	PDK4	Hs01037712_m1
Solute carrier family 2 (facilitated glucose transporter), member 4	SLC2A4	Hs00168966_m1

Table 3: List of SYBR green primers used in Study III.

Gene name	Gene ID	Forward sequence	Reverse sequence
F-box protein 32	Fbxo32 (Mafbx)	CACATCCCTGAGTGGCATC	CACATCCCTGAGTGGCATC
Insulin-like growth factor 1	Igf1	TGGATGCTCTTCAGTTCGTG	GCAACACTCATCCACAATGC
Myostatin	Mstn	ACGCTACCACGGAAACAATC	AAAAGCAACATTTGGGCTTG
PGC1α, isoform 4		TCACACCAAACCCACAGAAA	CTGGAAGATATGGCACAT
TATA box binding protein	Tbp	CCTTGTACCCTTCACCAATGAC	TCCTTCACCTGGTGGCTATT
Tripartite motif-containing 63	Trim63 (Murf1)	GCAAAGCATCTTCCAAGGAC	TCCTTCACCTGGTGGCTATT

3.6 PROTEIN ABUNDANCE ANALYSIS

Human and mouse skeletal muscle samples were homogenized in ice-cold homogenization buffer (20 mM Tris, pH 7.8, 137 mM NaCl, 2.7 mM KCl, 1 mM $MgCl_2$, 0.5 mM Na_3VO_4, 1% Triton X-100, 10% glycerol, 10 mM NaF, 0.2 mM phenylmethylsulfonyl fluoride, 1 mM EDTA, 5 mM $Na_4P_2O_7$, 1% (v/v) Protease Inhibitor Cocktail (Calbiochem, Darmstadt, Germany)) homogenized using either a motor-driven pestle (Polytron, Kinematica, Kriens, Switzerland) or the Tissue Lyzer II (Qiagen). Muscle lysates were subsequently rotated for 1 hour at 4°C and subjected to centrifugation at 12,000 g for 10 min at 4°C. The supernatant was collected and protein concentration was determined using a bicinchoninic acid protein assay kit (Pierce). Protein lysates were subsequently diluted into Laemmli buffer and heated for 20 min at 56°C. Equal amounts of protein were separated on precast Criterion SDS-PAGE gradient gels (Bio-Rad, Hercules, USA) and transferred to polyvinylidene difluoride membranes (Immobilion, Merck Millipore, Billerica, MA, USA). Membranes were blocked in 7.5% milk in Tris buffered saline-Tween (TBST, 0.05-0.1%) for 1 hour and incubated overnight with a primary antibody at 4°C. Membranes were washed and incubated with the appropriate horseradish peroxidase-conjugated secondary antibody (Bio-Rad) in 5% milk for 1 hour at room temperature. Proteins were visualized using enhanced chemiluminescence Western blotting detection reagents from GE Healthcare (Waukesha, WI, USA). Optical density of the bands was quantified using either

ImageJ image processing program (**Study I**) or Quantity One imaging system (Bio-Rad, **Study II and III**). All primary antibody dilutions were 1:1000, except for α-actinin 2 (1:250,000). Antibodies are listed in Table 4.

Table 4: List of antibodies used in Study I, II and III.

Antibody	Phosphory-lation site	Catalogue number	Manufacturer	Study
4E-BP1		9644	Cell Signaling	III
α-actinin 2			Gift from K. North	II
α-actinin 3			Gift from K. North	II
ACC		3662	Cell Signaling	III
Akt		9272	Cell Signaling	III
AMPKα		2532	Cell Signaling	III
AMPKα1			Gift from G. Hardie	III
AMPKα2		07-363	Merck Millipore	III
Beta-actin		A5441	Sigma-Aldrich	I
GAPDH		sc-25778	Santa Cruz	I, II
IκBα		9242	Cell Signaling	I
LC3I-II		L8918	Sigma-Aldrich	III
OXPHOS		ab110411	Abcam	II
mTOR		2983	Cell Signaling	III
MyHC-1		BA-D5	DSHB	II
MyHC-2A		SC-71	DSHB	II
MyHC-2B		BF-F3	DSHB	II
p62		P0067	Sigma-Aldrich	III
phospho-4E-BP1	$Thr^{37/46}$	9459	Cell Signaling	III
phospho-ACC	Ser^{79}	3661	Cell Signaling	III
phospho-Akt	Ser^{473}	9271	Cell Signaling	I, III
phospho-Akt	Thr^{308}		Cell Signaling	I
Phospho-AMPK	Thr^{172}	2531	Cell Signaling	III
phospho-IRS1	Tyr^{612}	44-816	Invitrogen	I
phospho-IRS1	Ser^{312}	07-247	Merck Millipore	I
Phospho-mTOR	Ser^{2448}	5536	Cell Signaling	III
phospho-PRAS40	Thr^{246}	44-1100	Invitrogen	I
phospho-S6 ribosomal protein	$Ser^{235/6}$	2217	Cell Signaling	III
phospho-TSC2	Thr^{1387}	5584	Cell Signaling	III
phospho-TSC2	Thr^{1462}	3617	Cell Signaling	III
S6 ribosomal protein		2217	Cell Signaling	III
SOCS3		2923	Cell Signaling	I

3.7 MEASUREMENT OF CYTOKINES AND METABOLITES

3.7.1 Cytokines

In **Study I**, serum levels of cytokines IL6 and IL8 were determined using the Milliplex Map assay from Merck Millipore (HSCYTO-60SK). In fully differentiated myotubes, release of IL6 and IL8 in cell media was measured using ELISA kits (Invitrogen). Myotubes were serum-starved overnight and medium was collected and frozen at -80°C. Samples were then thawed on ice and subjected to centrifugation for 15 min at 4°C. IL6 and IL8 concentration was determined according to the manufacturer's instructions using 100 µL of media.

3.7.2 Lactate release

For **Study I**, the lactate concentration in the cell media of fully differentiated myotubes was measured using a lactate colorimetric assay kit (Biomedical Research Service Center, State University of New York at Buffalo, NY, USA). Myotubes were serum-starved overnight and medium was collected and frozen at -80°C. Frozen aliquots of culture medium were thawed on ice. Twenty µL of sample were incubated for 60 min with lactate assay solution to initiate the enzymatic reduction of the tetrazolium salt INT, which produces a red formazan dye whose intensity is proportional to the lactate concentration. The reaction was then stopped by the addition of 3% acetic acid and the optical density is read at a wavelength of 492 nm.

3.7.3 Skeletal muscle glycogen content

In **Study III**, glycogen content in plantaris muscle was determined using a colorimetric commercially available kit (Abcam), according to the manufacturer's instructions. Briefly, 10 mg of muscle was homogenized into 200 µL of deionized water. Samples were subsequently boiled for 5 min to inactivate enzymes and subsequently subjected to centrifugation at 13,000 rpm for 5 min. Five µL of the supernatant was then pipetted into the plate and glucoamylase enzyme was added to hydrolyse glycogen into glucose. Produced glucose was subsequently oxidized for 30 min in the presence of OxiRed, a hydrogen peroxide probe. Finally, the optical density was read at a wavelength of 570 nm.

3.8 STATISTICAL ANALYSIS

All statistical analysis were performed using Graphpad or SPSS. Significance was set at $P < 0.05$. Data are presented as mean ± SEM.

3.8.1 Study I

Differences in anthropometric measurements and clinical parameters between before and after surgery were determined using a two-tail paired Student's t-test. The differences between cell cultures established before and after gastric bypass surgery were analyzed using either a two-tail paired Students t-test or a Wilcoxon matched pairs test. Cell culture metabolic measurements were analyzed with a Student t-test or ANOVA when appropriate.

3.8.2 Study II

Differences in anthropometric measurements and clinical parameters between NGT and T2D (**Paper II**, Table 1) were assessed using two-tail Student's t-test or a Mann-Whitney U-test when the data were not normally distributed. For genotype distribution, Hardy-Weinberg equilibrium was tested using the Chi-squared test (**Paper II**, Table 2). Anthropometric measurements and clinical parameters in relation to genotype (**Paper II**, Table 3) were analyzed with a Kruskal-Wallis test to evaluate differences between groups. Gene expression and Western blot quantification analysis (**Paper II**, Fig. 1 to 3) were performed using two-way ANOVA to examine both effects of genotype and glucose tolerance status. Pairwise *post hoc* comparisons were determined using Bonferroni correction to control for type 1 errors.

3.8.3 Study III

All data was analyzed using two-way ANOVA to examine both effects of genotype and intervention. Pairwise *post hoc* comparisons were determined using Bonferroni correction to control for type 1 errors.

4 RESULTS AND DISCUSSION

4.1 STUDY I

Surgical procedures such as RYGB rapidly improve whole-body glucose homeostasis and leads to a progressive, sustainable loss of fat mass. Skeletal muscle contributes to the improved whole-body insulin sensitivity following RYGB. Using a longitudinal *in vitro* model, the effects RYGB on glucose and lipid metabolism, insulin signaling and inflammation markers in primary human myotubes was determined. This *in vitro* model allows for a direct comparison between metabolic and signaling responses in cultures obtained before and after RYGB.

4.1.1 Changes in clinical parameters six months after RYGB

Since the subjects had an average BMI of 41.8 kg/m^2, they were eligible for RYGB. Anthropometric and metabolic characteristics were measured before and 6 months after the intervention. RYGB decreased initial body weight by 25%, which is typical in the case of this specific bariatric surgery procedure (Madsbad *et al.*, 2014). Although patients were not diabetic, RYGB improved fasting blood glucose and insulin levels (**Paper I**, Table 1).

4.1.2 Effects of RYGB on mRNA of myogenic markers

In order to orchestrate myogenesis and myotube formation, several genetic factors vary temporally during the proliferation and the differentiation process (Bentzinger *et al.*, 2012). To determine if RYGB alters the capability of myoblasts to differentiate, mRNA expression of myogenic markers, including proliferative markers paired-box 3 and 7 (PAX3-7), MyoD, myogenin and desmin, was determined in myoblasts and differentiated myotubes isolated from muscle biopsies taken from the study volunteers before and after RYGB (**Paper I**, Fig. 1A). As expected, expression level of the proliferative marker PAX7 decreased, while those of myogenin and desmin increased during differentiation. Expression levels of MyoD, a transcription factor that drives cell commitment to differentiate by activating transcription of muscle-specific genes (Rudnicki *et al.*, 1993), and

PAX3 were unchanged with differentiation. Together these data indicate that all the cell cultures underwent differentiation. Myoblasts isolated post-RYGB had increased gene expression of PAX3, PAX7, myogenin and desmin compared to those isolated pre-RYGB, suggesting an enhanced cell commitment potential of the myoblasts. The expression of myogenic markers was unaltered between myotubes derived from pre- and post-RYGB muscle biopsies (**Paper I**, Fig. 1B). Furthermore, a genetic component may be at work as differentiation-induced changes in gene expression were more similar in individuals within pre- and post-RYGB, as compared across different donors (Fig. 8).

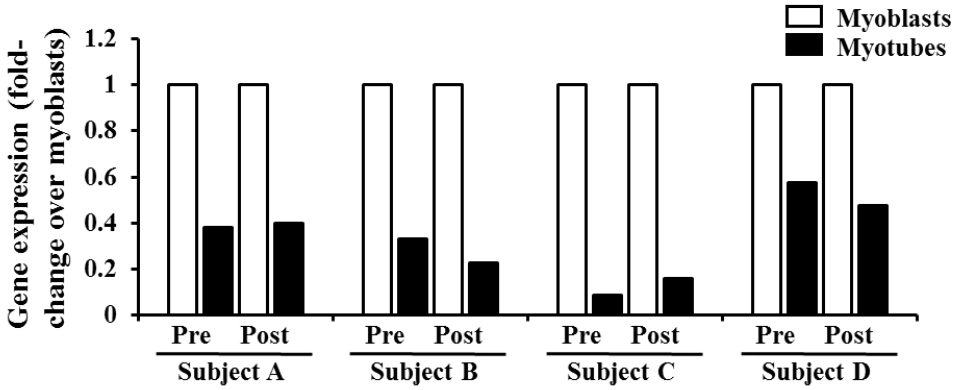

Figure 8: Fold-change in gene expression is preserved in pre and post-gastric bypass surgery cell cultures. Changes in PAX7 gene expression following differentiation in individual subjects before gastric bypass surgery (Pre) and 6 months after gastric bypass surgery (Post).

4.1.3 Glucose, but not lipid metabolism, is improved following RYGB

Improvements in peripheral glucose and lipid metabolism could contribute to restored whole-body metabolic homeostasis following RYGB. Rates of insulin-stimulated glucose transport in isolated skeletal muscle strips obtained from patients who underwent RYGB are improved compared to extremely obese or weight-matched individuals (Friedman *et al.*, 1992; Bikman *et al.*, 2008). To investigate the fate of glucose as energy substrate in human muscle cells derived from biopsies taken before and after RYGB, basal and insulin-stimulated glucose incorporation into glycogen was assessed. Basal, but not insulin-stimulated, glucose incorporation into glycogen was improved in the post-surgery myotubes

when compared to their matched pre-RYGB cultures (**Paper I**, Fig. 2A). The mRNA expression of selected genes involved in glucose metabolism, including genes encoding for glucose transporter GLUT4, were not altered by surgery (**Paper I**, Fig. 2D), consistent with results in isolated skeletal muscle strips (Friedman *et al.*, 1992). These results suggest that improvements in glucose handling after surgery do not result from transcriptional changes in these targets. As human skeletal muscle cells express low levels of GLUT4 (Sarabia *et al.*, 1992), alterations in insulin signaling may be a better metric of insulin-induced alterations.

The activity of IRS1 is reciprocally regulated by tyrosine and serine phosphorylation. While tyrosine phosphorylation allows IRS1 to bind to PI3K and activate the downstream insulin signaling cascade, serine phosphorylation is regarded as inhibitory (Gual *et al.*, 2005). In myotubes obtained post-RYGB, basal phosphorylation of IRS1 was potentiated at Tyr^{612} while Ser^{312} phosphorylation was not changed (**Paper I**, Fig. 4C). A decrease in basal IRS1 Ser^{312} phosphorylation has been reported in muscle strips taken from patients 12 months after RYGB, compared to weight-matched controls and extremely obese individuals (Bikman *et al.*, 2008). Downstream of IRS1, insulin signaling was potentiated in cell cultures obtained post-RYGB versus pre-RYGB. Insulin-stimulated phosphorylation of Akt at Thr^{308} and PRAS40 at Thr^{246} was increased following surgery (**Paper I**, Fig. 4A-B). In human skeletal muscle cells and mouse skeletal muscle, overexpression of PRAS40 enhances insulin sensitivity, likely by increasing protein abundance of IRS1 and potentiating Akt phosphorylation at Thr^{308} (Wiza *et al.*, 2014). This mechanism could be reproduced in the post-RYGB cell cultures and may contribute to the restoration of glucose homeostasis in skeletal muscle following RYGB. Collectively, these data provide evidence that RYGB improves glucose disposal and glycogen storage into skeletal muscle cells by potentiating phosphorylation of key insulin signaling intermediates.

Skeletal muscle metabolic inflexibility in lipid handling as displayed by obese individuals is maintained *in vitro*. Lipid utilization in response to lipid exposure was not increased in myotubes derived from skeletal muscle of obese

individuals compared to myotubes derived from muscle of healthy individuals (Boyle *et al.*, 2012). In individuals who underwent RYGB, the contribution of lipids to energy expenditure at rest and during exercise is lower than in age-matched females who have never been obese, even two years after the surgical intervention (Guesbeck *et al.*, 2001). To test the effect of RYGB on the ability to increase reliance on lipid as energy substrate at the myotube level, fatty acid oxidation, using low (20 μM) and high (500 μM) doses of palmitate, was measured. Fatty acid oxidation remained unchanged under low and high doses of lipid supply between the pre- and post-RYGB conditions (**Paper I**, Fig. 2B-C). Similarly, mRNA expression of specific genes involved in lipid handling were unaltered (**Paper I**, Fig. 2D). Thus, *in vitro* and *in vivo* data from both cross-sectional and longitudinal studies suggest that obesity-related defects in the use of lipids as energy substrate is inherent to the skeletal muscle cell and insensitive to RYGB. Moreover, this metabolic inflexibility of the muscle cell and inability to increase the use of lipids as energy substrate might facilitate or pre-dispose to regain weight.

4.1.4 Effects of RYGB on inflammatory markers

Chronic low-grade inflammation is a characteristic of excess body weight and metabolic inflexibility. There is accumulating evidence for crosstalk between the immune cells and skeletal muscle (Pillon *et al.*, 2013). Since weight-loss strategies improve the inflammatory profile (Imayama *et al.*, 2012), we measured IL6 and IL8 release into cell media in pre- and post-RYGB cell cultures. We also compared the *in vitro* levels of these cytokines to the plasma levels detected in the patients. Six months after RYGB, IL6 and IL8 levels remained unchanged (**Paper I**, Table I). However, IL8 secretion was increased *in vitro*, following RYGB (**Paper I**, Fig. 3A). To verify that IL8 did not mediate the changes in glycogen synthesis, post-RYGB myotubes were treated with IL8 and glucose incorporation into glycogen was measured. IL8 did not affect glycogen synthesis (**Paper I**, Fig. 3C). IL8 was also without effects on palmitate oxidation (**Paper I**, Fig. 3D). Consistent with unchanged IL6 levels between the pre- and the post-RYGB cultured cells, SOCS3 protein abundance was also unchanged. SOCS3 contributes

to the development of peripheral insulin resistance (Emanuelli *et al.*, 2000). Moreover, SOCS3 protein abundance is increased in skeletal muscle from T2D patients compared to weight-matched or lean individuals (Rieusset *et al.*, 2004; Mashili *et al.*, 2013), SOCS3 levels remained unchanged in skeletal muscle from obese individuals compared to lean controls (Rieusset *et al.*, 2004), which supports the present results. SOCS3 levels in the context of extreme obesity (BMI≥40 kg/m^2) and bariatric surgery had not been investigated and the results generated in this thesis provide further evidence that changes in SOCS3 levels are independent of obesity and likely to be related to insulin resistance. Finally, molecular signals regulating inflammation markers in the context of RYGB could also be a dynamic process that varies according to the time-point investigated, especially until a stable weight loss has been achieved.

4.1.5 Summary

Weight-loss surgery induces changes in whole-body metabolism and improvements in the metabolic regulation of local tissues such as skeletal muscle are likely to contribute to those changes. Improvements in peripheral insulin sensitivity and glucose disposal following RYGB have been postulated to be a consequence of caloric restriction and weight loss (Ferrannini & Mingrone, 2009; Dirksen *et al.*, 2012), but little work has actually been done to assess the local changes in skeletal muscle following RYGB. The *in vitro* results presented in this thesis provide further evidence for improved local glucose metabolism and insulin signaling in skeletal muscle and that the impaired glucose disposal in skeletal muscle of extremely obese patients is a reversible defect. To further strengthen the results from this study, studies of cell cultures from a lean cohort in parallel could provide additional valuable insight into the pathogenesis of insulin resistance in obesity. By investigating other time points following RYGB, such as 12 or 18 months, insight into the mechanism for improved peripheral insulin sensitivity may be revealed at a stage when the weight loss has progressed further.

4.2 STUDY II

The mechanism by which the ACTN3 R577X polymorphism impacts skeletal muscle performance is incompletely resolved and the influence of this gene variant on metabolic disease remains unexplored. This study has investigated the prevalence of the ACTN3 R577X SNP in a cohort of NGT, IGT and T2D subjects, as well as a possible association with metabolic traits, MyHC isoforms, mitochondrial enzymes of the electron transport chain and sarcomeric proteins.

4.2.1 Higher prevalence of the ACTN3 577XX genotype in T2D patients

The ACTN3 R577X polymorphism consistently associates to elite athletic performance, but its effect on metabolic disease is unknown. To address this question, a cohort of 211 male and female participants classified as NGT, IGT or T2D was genotyped for this common polymorphism. Body weight, waist circumference, BMI, fasting blood glucose, 2 hours blood glucose, HbA_{1c} levels, and homeostasis model assessment – estimated insulin resistance (HOMA-IR) levels were assessed in NGT, IGT and T2D participants (Table 5; **Paper II**, Table 1).

Departure from the Hardy–Weinberg equilibrium (HWE) was assessed using Pearson's chi-square test (Lewis & Knight, 2012). The genotype distribution of the complete cohort met the HWE, with the R and X allele reaching frequencies of 0.6 and 0.4, respectively (**Paper II**, Table 2). A higher frequency of the 577XX genotype was detected in individuals with T2D versus NGT (P=0.039; **Paper II**, Table 2). The distribution of the genotype among the NGT, IGT and T2D groups is shown (Table 6). The anthropometric and metabolic parameters of the participants were unrelated to the ACTN3 genotype across glucose tolerance status (Table 7; **Paper II**, Table 3), suggesting that the ACTN3 genotype does not impact metabolic phenotype. In contrast with another clinical study in women across the adult lifespan (Walsh *et al*., 2008), genotype and BMI were not related in this study, although both men and women were included in our analysis.

Table 5: Anthropometric and metabolic traits of the study participants.

	NGT	IGT	T2D	*P* value
n	128	34	49	
Sex (M/F)	47/81	15/19	31/18	
Age (y)	59±1	61±1	61±1	n.s.
Height (cm)	170±1	171±1	172±1	n.s.
Weight (kg)	84.7±1.0	89.4±2.1	92.8±2.1$^{\#}$	<0.01
Waist circumference (cm)	98.2±0.9	102.4±1.6	104.6±1.5$^{\#}$	<0.01
BMI (kg/m^2)	29.5±0.3	30.9±0.7	31.4±0.6$^{\#}$	<0.05
Fasting glucose (mmol/l)	5.5±0.0	5.8±0.1	7.9±0.2$^{\#\S}$	<0.001
2-h glucose (mmol/l)	7.2±0.1	10.1±0.2*	15.4±0.6$^{\#}$	<0.001
Insulin (pmol/l)	57.5±3.0	69.3±10.0	69.5±6.2	n.s.
HbA1c (%)	4.7±0.0	4.9±0.1	6.1±0.1$^{\#\S}$	<0.001
HOMA-IR	2.0±0.1	2.6±0.4	3.5±0.3$^{\#\S}$	<0.001
Workload (W)	157±4	155±7	158±5.5	n.s.
Oxygen uptake	24.0±0.6	22.3±1.0	22.9±1.0	n.s.

Data are mean±SEM. HOMA-IR, homeostasis model assessment – estimated insulin resistance; W, watts. Oxygen uptake presented as ml x min^{-1} x kg^{-1}. Statistical comparison between groups was determined using a Kruskal–Wallis test. Pairwise comparison post-hoc analysis with Bonferroni correction was used to detect differences between groups. Significant differences (P < 0.05) are indicated as * NGT vs. IGT; # NGT vs. T2D; § IGT vs. T2D.

Table 6: ACTN3 genotype distribution among NGT, IGT and T2D.

		n	***n***			**%**		
		All	**577RR**	**577RX**	**577XX**	**577RR**	**577RX**	**577XX**
NGT		**128**	51	61	16	41	47	12
IGT		**34**	14	13	7	39	39	21
T2D		**49**	11	26	12*	22	53	24
Total		**211**	**76**	**100**	**35**	**33**	**47**	**17**

577RR: homozygous wild-type, 577RX: heterozygous, 577XX: homozygous null. *P < 0.05 for T2D vs. NGT and IGT.

Deviations from the HWE can also occur if assumptions are not fulfilled. For example, it was assumed that the cohort was of unrelated ancestry, although it is unknown if the individuals were unrelated to each other for several generations. Genotyping studies generally use large cohorts since a small cohort could be non-representative of the population, possibly leading to genetic drift and derivation

from the HWE equilibrium. When this is the case, validating the genotyping results using Fisher's Exact Test is a useful alternative and may even prove to be more accurate. Fisher's Exact Test confirmed our findings (P= 0.01) strengthening the data despite the absence of correlations or associations between genotype and measured anthropometric and metabolic parameters. For further molecular readouts analyses, IGT individuals were removed from the analysis because of limitations in starting material.

Table 7: Association between ACTN3 R577X genotype with anthropometric and metabolic traits.

	NGT			IGT			T2D		
Genotype	RR	RX	XX	RR	RX	XX	RR	RX	XX
n	51	61	16	14	13	7	11	26	12
Sex (M/F)	21/30	20/41	6/10	7/7	5/8	3/4	37/39	16/10	6/6
Age (y)	60±1	60±1	56±2	61±2	61±2	62±2	58±2	63±1	60±1
Weight (kg)	85.9±1.9	84.0±1.3	83.9±3.2	94.2±3.0	88.9±3.2	80.8±4.2	94.4±4.0	93.7±3.1	89.2±3.8
Waist (cm)	99.0±1.5	98.3±1.1	95.1±2.7	104.5±2.0	103.2±2.7	96.7±3.7	103.8±2.2	105.1±2.4	104.1±2.8
BMI (kg/m^2)	29.5±0.4	29.5±0.4	29.2±1.0	31.8±1.1	31.2±1.1	28.7±1.1	30.5±1.0	31.7±0.9	31.8±1.4
f-glucose (mmol/l)	5.4±0.1	5.5±0.1	5.6±0.1	5.7±0.2	5.9±0.2	5.6±0.2	8.1±0.7	7.8±0.2	8.0±0.5
2-h glucose (mmol/l)	7.2±0.1	7.2±0.1	7.1±0.2	10.1±0.2	10.2±0.3	10.1±0.4	15.3±1.4	14.6±0.7	16.9±1.1
f-insulin (pmol/l)	62.4±5.2	56.8±4.5	43.8±4.4	70.8±33.8	54.3±12.5	82.3.1±12.7	80.8±16.8	62.9±7.6	72.9±9.1
HbA_{1c} (%)	4.7±0.1	4.7±0.1	4.6±0.1	4.9±0.1	4.9±0.1	4.8±0.1	6.2±0.4	6.0±0.2	6.2±0.2
HOMA-IR	2.2±0.2	2.0±0.2	1.6±0.2	3.0±0.5	2.1±0.5	2.5±1.2	4.0±0.8	3.1±0.4	3.8±0.5
Workload (W)	163±6	150±5	166±11	165±9	150±11	149±21	171±12	155±8	155±8
Oxygen Uptake	24.3±0.9	23.3±0.9	25.9±1.7	20.0±1.5	22.3±1.7	23.5±1.6	24.5±1.8	21.6±1.5	24.4±1.6

Data are mean±SEM. HOMA-IR, homeostatic model assessment - insulin resistance; W, watts. Oxygen Uptake values are presented as mL x min^{-1} x kg^{-1}. Statistical comparison of genotype within groups was performed using the Kruskal–Wallis test.

4.2.2 Influence of ACTN3 R577X genotype on metabolism

A lack of α-actinin 3 protein could modulate substrate utilization and storage in skeletal muscle of the ACTN3$^{-/-}$ mice (MacArthur *et al.*, 2007; Quinlan *et al.*, 2010). However, these results in ACTN3$^{-/-}$ mice could not be reproduced in humans (Vincent *et al.*, 2012; Norman *et al.*, 2014). To explore a direct relationship between the ACTN3 R577X polymorphism and energy substrate in the muscle cell, glucose incorporation into glycogen and beta-oxidation of palmitic acid was assessed in differentiated human skeletal muscle cells derived from skeletal muscle of α-actinin 3-expressing (577RR, 577RX) or null (577XX) individuals. ACTN2 and ACTN3 expression during differentiation process was also assessed (Fig. 9).

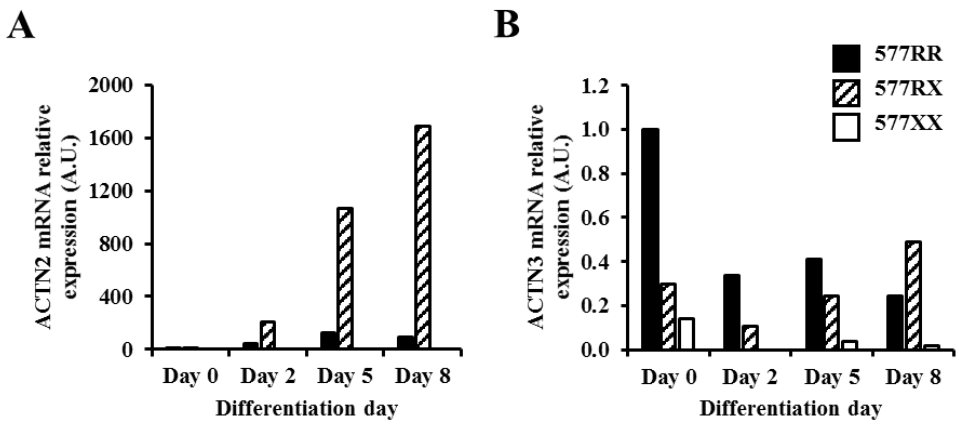

Figure 9: mRNA expression of muscle-specific α-actinin isoforms in *vastus lateralis* muscle from NGT and T2D subjects. A) ACTN2 and B) ACTN3 in primary human myotubes carrying the 577RR, 577RX, and 577XX ACTN3 genotype. Results are normalized to B2M mRNA and presented as mean±SEM.

Basal and insulin-stimulated glucose incorporation into glycogen were unaltered between genotypes (Fig. 10). Similarly, beta-oxidation of palmitic acid was also unchanged between genotypes (Fig. 10). In the ACTN3$^{-/-}$ mouse, changes in enzyme activity cannot be detected before week 4 of age (Quinlan *et al.*, 2010). Thus, skeletal muscle cells may not fully resemble functional and contracting adult skeletal muscle to adequately display a phenotype similar to the one of genetically engineered ACTN3$^{-/-}$ mouse. The differences in studying the role of ACTN3 in

cultured cells versus fully differentiated adult muscle could account for unchanged energy substrate handling in the myotubes, despite the presence or absence of the R577X polymorphism.

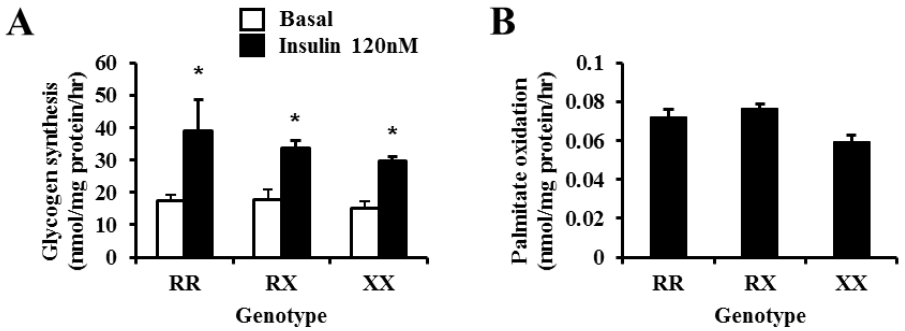

Figure 10: Glucose incorporation into glycogen and lipid oxidation in human myotubes. A) Basal and insulin-stimulated glucose incorporation into glycogen. B) Palmitate beta-oxidation. RR: 577RR wild-type homozygous; RX 577RX heterozygous; XX: 577XX wild-type null. n = 3 experiments. Results are mean±SEM. * $P \leq 0.01$ indicates insulin effect.

4.2.3 Influence of ACTN3 R577X genotype on α-actinin levels in people with NGT or T2D

ACTN3$^{-/-}$ mice displays higher levels of α-actinin 2 in skeletal muscle (MacArthur *et al.*, 2007; Seto *et al.*, 2013). To evaluate whether T2D status interacts with ACTN3 R577X genotype to impact levels of α-actinin, gene expression and protein abundance of muscle-specific α-actinin isoforms from *vastus lateralis* muscle biopsies of NGT or T2D individuals carrying the different ACTN3 R577X genotypes were measured (**Paper II**, Fig. 1). ACTN3 mRNA followed the expected allele-dependent expression pattern in both NGT and T2D. Although α-actinin 2 protein abundance is increased in ACTN3$^{-/-}$ mice, the present thesis work and a previous study (Norman *et al.*, 2009) provide evidence for unaltered α-actinin 2 mRNA and protein, irrespective of genotype and glucose tolerance status. As there is greater sequence homology (>80%) between α-actinin 2 and α-actinin 3 in humans than in mice (Mills *et al.*, 2001), functional redundancy could mask a phenotype possibly arising from an ACTN3 deficiency in humans (Beggs *et al.*, 1992). Conversely, the high prevalence of the 577XX

genotype in the general Caucasian population (16-18%) argues against a pathogenic role for this polymorphism (North *et al.*, 1999). While α-actinin 2 is expressed in all skeletal muscle fiber types, the expression of α-actinin 3 is specific to glycolytic type II muscle fibers (North & Beggs, 1996). Humans have 40-50% of type 2 glycolytic fibers, but in mice, this percentage rises to 80% (Agbulut *et al.*, 2003; Schiaffino & Reggiani, 2011). Inter-species differences in isoform homology and fiber type composition could perhaps explain why other ACTN3 isoform failed to compensate for the ACTN3 deficiency in human *vastus lateralis* muscle biopsies.

4.2.4 Protein abundance of myosin heavy chain isoforms and components of the mitochondrial electron transport chain

α-actinin 3 gene expression is restricted to type II glycolytic muscle fibers. Thus, the impact of the ACTN3 R577X polymorphism could impact muscle fiber type composition (Vincent *et al.*, 2007; MacArthur *et al.*, 2008; Norman *et al.*, 2009). Only one study reports an increase in the percentage of type IIB fibers in individuals carrying the 577RR genotype (Vincent *et al.*, 2007). In the cohort studied in this thesis, the ACTN3 R577X polymorphism did not influence protein abundance of the different myosin heavy chain isoforms as evaluated by Western blot (**Paper II**, Fig. 2), consistent with other clinical reports (Norman *et al.*, 2009; Norman *et al.*, 2014). Furthermore, skeletal muscle fiber type distribution is unaltered between untrained $ACTN3^{-/-}$ and wild-type mice, despite the presence of a shift towards oxidative properties (MacArthur *et al.*, 2008; Seto *et al.*, 2013), thereby uncoupling the ACTN3-induced metabolic improvements from fiber type changes. Interestingly, an interaction between glucose tolerance status and both MyHC-1 and MyHC-2a was detected in the present material, with T2D patients displaying increased protein abundance of these markers compared to NGT individuals. This finding was unexpected, since the proportion of glycolytic skeletal muscle fibers is increased in T2D patients compared to NGT subjects, while MyHC-1 abundance is reduced (Oberbach *et al.*, 2006; Larsen *et al.*, 2011). Despite the increase in MyHC-2A protein abundance, α-actinin 3 level was unaltered in T2D patients. Protein abundance of mitochondrial transport chain enzymes specific for complex I, III and IV was reduced in skeletal muscle from

T2D patients compared to NGT, consistent with previous work (Oberbach *et al.*, 2006; Larsen *et al.*, 2011). An interaction between genotype and glucose tolerance status for protein abundance of NDUFB8 (complex I) and COX2 (complex IV) could be detected: the abundance of these oxidative enzymes was increased with the number of X alleles in NGT individuals, whereas an inverse relationship was noted in T2D patients. Collectively, the data in this thesis provides evidence to suggest that the 577XX genotype is insufficient to protect against the decreased abundance of oxidative enzymes characteristic of T2D.

4.2.5 Influence of ACTN3 577XX genotype on mRNA expression of sarcomeric proteins

α-Actinin proteins function to stabilize and preserve the integrity of the sarcomere through interactions with other sarcomeric proteins localized at the Z-line. In ACTN3$^{-/-}$ mice, mRNA and protein level of a subset of sarcomeric proteins is upregulated, providing evidence that the absence of α-actinin 3 can alter the z-line composition of the sarcomere (Seto *et al.*, 2011). To determine if the absence of α-actinin 3 is also associated to an altered expression profile of sarcomeric proteins in human skeletal muscle, mRNA abundance of a selected subset of sarcomeric α-actinin 3-interacting proteins in skeletal muscle from healthy NGT individuals was quantified. Consistent with previous work in ACTN3$^{-/-}$ mice, myotillin and PDZ and LIM domain 3 (PDLIM3) mRNA expression was up-regulated in human skeletal muscle from 577XX NGT individuals compared to muscle from 577RR individuals. Extending the mRNA screening to other Z-line-specific proteins known to interact with α-actinin, revealed similar changes in actin, capping proteins, calsarcins (or myozenins), as well as giant molecular rulers nebulin and titin (**Paper II**, Fig. 4). Increased α-actinin 2 expression in skeletal muscle from ACTN3$^{-/-}$ mice competes with the calcium- and calmodulin-dependant protein phosphatase calcineurin to bind calsarcin, resulting in increased calcineurin signaling (Seto *et al.*, 2013). This endogenous over-activation of the calcineurin pathway could alter the downstream regulation of transcription factors, such as NFAT, leading to a shift towards a more oxidative phenotype in skeletal muscle fibers. Even though ACTN2 is not upregulated in α-actinin 3-deficient human skeletal muscle, calsarcins remain an attractive candidate to solve the

molecular mechanism by which the deficiency of α-actinin 3 influences skeletal muscle performance. Since other genes encoding for proteins interacting with calsarcins, such as myotilin are up-regulated, the reduced inhibition activity of calsarcin-2 may also be potentiated by other sarcomeric proteins.

4.2.6 Summary

The ACTN3 R577X common polymorphism is the gene variant most consistently associated with skeletal muscle performance (Eynon *et al.*, 2013). Nevertheless, the role the ACTN3 R577X polymorphism has never been addressed in the context of metabolic diseases until now. The results presented in **Study II** provide evidence to suggest that this polymorphism does not pose a strong genetic risk toward the development of metabolic disease, despite a higher prevalence of the 577XX genotype in people with T2D vs. NGT. Rather than altering metabolic regulation, the absence of α-actinin 3 due to the ACTN3 577XX genotype could influence muscle performance by up-regulating several sarcomeric genes as a compensation mechanism to the lack of α-actinin 3, independent of alterations in α-actinin 2 expression.

4.3 STUDY III

There is evidence for a crosstalk between AMPK and mTOR in the context of the regulation of cell size. The isoforms of the different AMPK subunits, including the γ3 isoform, could modulate the hypertrophic response to functional overload. This study addresses this question by looking into functional, transcriptional and signaling responses in skeletal muscle of γ3 genetically modified mouse models after a 14-day functional overload.

4.3.1 Role of the AMPK γ3 isoform on the hypertrophy response in skeletal muscle

Skeletal muscle hypertrophy in Tg-Prkag3^{225Q} and Prkag3$^{-/-}$ mice was induced by functional overload using the synergistic muscle ablation model. To confirm that this model induced hypertrophy, plantaris muscle weight from both

overloaded and control sham-operated mice were compared. Tg-Prkag3^{225Q}, Prkag3$^{-/-}$ and wild-type littermates displayed a robust increase in absolute and relative plantaris weight in response to overload compared to sham-operated mice and thus underwent hypertrophy (**Paper III**, Fig. 1). In Tg-Prkag3^{225Q} mice, the plantaris of sham-operated mice were heavier compared to wild-type mice. However, this difference was not preserved following functional overload, indicating that wet weight gain in the plantaris muscle of Tg-Prkag3^{225Q} mice was reduced compared to wild-type counterparts (**Paper III**, Fig. 1G).

4.3.2 Transcriptional response to overload in Tg-Prkag3^{225Q} and Prkag3$^{-/-}$ mice

To test whether the expression of markers characteristic of skeletal muscle hypertrophy and atrophy followed the same response as the wet muscle mass, mRNA expression of pro-atrophic genes encoding for myostatin and E3 ubiquitin ligases Murf1 and Mafbx, as well as hypertrophic genes Igf1 and Pgc1α isoform 4 (PGC1α4), a splice variant originating from the alternative promoter of Pgc1α (Ruas *et al.*, 2012) was determined. Following functional overload, transcript abundance of Igf1 was increased, whereas mRNA of pro-atrophic markers were decreased, independently of genotype (**Paper III**, Fig. 2). However, in plantaris of Tg-Prkag3^{225Q} control sham-operated animals, Igf1 mRNA was reduced compared to wild-type. (**Paper III**, Fig. 2A). As expected, all the pro-atrophic genes were down-regulated with functional overload in all genotypes. Furthermore, no genotype effect could be detected in the sham-operated animals.

Pgc1α4 transcript expression was decreased in wild-type mice in response to overload, but unchanged in Tg-Prkag3^{225Q} and Prkag3$^{-/-}$ mice (Fig. 11). This finding is consistent with earlier work showing that expression of PGC1α4 remains unchanged following functional overload (Perez-Schindler *et al.*, 2013). Moreover, skeletal muscle overload hypertrophy is unaffected by the absence of Pgc1-α (Perez-Schindler *et al.*, 2013). Since skeletal muscle from both Tg-Prkag3^{225Q} and Prkag3$^{-/-}$ mice undergo normal overload hypertrophy, despite unchanged or reduced Pgc1-α4 transcript abundance, this evidence further suggests that the splice variant Pgc1-α4 is not involved in the hypertrophic

response following 14-day functional overload. Together, these transcriptional data are consistent with the present finding that the AMPK γ3 isoform is dispensable for the hypertrophic response in skeletal muscle.

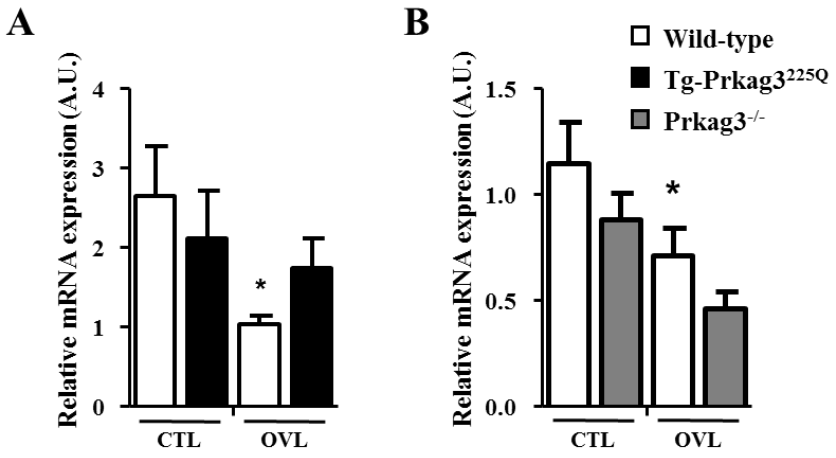

Figure 11: mRNA expression of splice variant PGC1α4 A) Tg-Prkag3^{225Q} vs. wild-type B) Prkag3$^{-/-}$ vs. wild-type. Results are normalized to Tbp mRNA and presented as mean±SEM. *n*=6-9/genotype/treatment. **P*<0.05 for Tg-Prkag3^{225Q} or Prkag3$^{-/-}$ vs. wild-type. #*P*< 0.05 for control (CTL) vs. overload (OVL).

4.3.3 Impact of the γ3 isoform of AMPK on mTOR signalling cascade

To gain further insight into the role of the γ3 isoform of AMPK in the hypertrophic response, phosphorylation and total abundance of signaling intermediates of the mTOR pathway were measured in plantaris muscle from Prkag3^{225Q} and Prkag3$^{-/-}$ mice. This pathway conveys signal transduction leading to increased protein synthesis and muscle hypertrophy (Egerman & Glass, 2014). mTOR signaling is altered in AMPKα1$^{-/-}$ mice undergoing 7 or 21 days of functional overload (Mounier *et al.*, 2009). In all genotypes, phosphorylation and total abundance of Akt and mTOR, as well as downstream effectors of p70S6 kinase RPS6 and 4E-BP1 were increased in plantaris muscle by overload (**Paper III**, Fig. 3-4). This result indicates that the hypertrophy signaling pathway, ultimately leading to protein synthesis and cell growth, is similarly activated

following functional overload and provides further evidence that the AMPK γ3 isoform is dispensable for skeletal muscle hypertrophy.

4.3.4 AMPK signaling following overload-induced hypertrophy in Tg-Prkag3^{225Q} and Prkag3$^{-/-}$ mice

Since the gain-of-function R225Q mutation in the γ3 isoform confers increased basal constitutive activation of AMPK in EDL muscle of Tg-Prkag3^{225Q} mice (Barnes *et al.*, 2004), the effects of functional overload on AMPK signaling were assessed in plantaris muscle from Tg-Prkag3^{225Q} and Prkag3$^{-/-}$ mice. Phosphorylation on Thr^{172} site of the α catalytic subunit of AMPK was robustly decreased following overload in Tg-Prkag3^{225Q} and wild-type mice, irrespective of genotype (**Paper III**, Fig. 5A). This was accompanied by increases in total protein abundance of AMPKα, AMPKα1 and AMPKα2 with overload in Tg-Prkag3^{225Q} and wild-type mice (**Paper III**, Fig. 5B-C-D). Phosphorylation of AMPKα on Thr^{172} was unchanged in Prkag3$^{-/-}$ mice and increased in wild-type mice. AMPK phosphorylation in Tg-Prkag3^{225Q}, Prkag3$^{-/-}$ and wild-type littermates is similar under basal, AICAR stimulation or muscle contraction conditions (Barnes *et al.*, 2004). Moreover, Tg-Prkag3^{225Q} mice are resistant to further increases in AMPK activity induced by increasing levels of AMP. Previous studies using other genetic mouse models provide evidence that increased AMPK and ACC phosphorylation following overload can be attributed to increased AMPKα1 activity (McGee *et al.*, 2008; Perez-Schindler *et al.*, 2013). However, in this thesis work AMPK phosphorylation was decreased (in Tg-Prkag3^{225Q}) or unchanged (in Prkag3$^{-/-}$) following 14-day overload, despite an increase in AMPKα1 abundance in all genotypes. While this finding contrast earlier studies (McGee *et al.*, 2008; Perez-Schindler *et al.*, 2013), it is not entirely unexpected, since Akt and mTOR signaling is inversely correlated with AMPK signaling.

Differences in AMPK phosphorylation between Tg-Prkag3^{225Q} and Prkag3$^{-/-}$ mice could also be attributed to a different dynamic response to the synergistic ablation model. The differences in AMPK and ACC phosphorylation could be related to the time-point investigated (7, 14 or 21-day overload). Thus, genetic alteration of different AMPK isoforms is likely to be without an impact on

final muscle weight, but could affect the rate at which muscle growth occurs during the hypertrophy.

Increasing evidence suggests that AMPK plays a role in autophagy in the context of exercise (He *et al.*, 2012; Sanchez *et al.*, 2012). To gain further insight into the metabolic effects of functional overload on mechanism controlling autophagy, protein abundance of the autophagic markers p62 and LC3 were determined. While p62 was increased with overload, the LC3-I: LC3-II ratio was unchanged. Abundance of the autophagic markers was similar between genotypes, suggesting that the γ3 isoform of AMPK is dispensable for autophagosome formation.

4.3.5 Glycogen content

After acute exercise, skeletal muscle glycogen content readily increases when adequate carbohydrates are consumed in the recovery period (Bergstrom & Hultman, 1966). One of the most striking features of the Prkag3 R225Q polymorphism is the profound increase in glycogen content in glycolytic skeletal muscle at baseline and after exercise in pigs and mice harboring the mutation (Milan *et al.*, 2000; Barnes *et al.*, 2004; Barnes *et al.*, 2005a). Glycogen can account for 0.7% of skeletal muscle weight. Given that 3 to 4 grams of water are bound to each gram of glycogen (Olsson & Saltin, 1970), the increased glycogen content in skeletal muscle from the Tg-Prkag3^{225Q} mice may contribute to the increased plantaris mass in sham-operated Tg-Prkag3^{225Q} mice. Glycogen content was increased by 40% in control Tg-Prkag3^{225Q} mice compared to wild-type littermates, reflecting the effect of the mutation (**Paper III**, Fig. 8). Glycogen content was also increased in between Tg-Prkag3^{225Q} and wild-type mice following 14-day overload (**Paper III**, Fig. 8). Thus, the increase in water content may partly explain the 10% difference in plantaris wet mass between sham-operated Tg-Prkag3^{225Q} and wild-type animals.

4.3.6 Summary

Collectively, the results presented in this thesis provide evidence that the γ3 isoform of AMPK is dispensable for skeletal muscle hypertrophy. The

increased wet muscle mass of the plantaris muscle in Tg-Prkag3^{225Q} sham-operated mice compared to wild-type suggests that the rate at which skeletal muscle undergoes hypertrophy differs in Tg-Prkag3^{225Q} mice compared to wild-type littermates. To solidify this finding, a time-course experiment with 7-day and 21-day endpoints could have proven valuable, especially considering the potentiated hypertrophic response of AMPK$\alpha 1^{-/-}$ mice in response to functional overload. Direct measurement of AMPK activity under sham-operated and overload conditions would also clarify the understanding of AMPK signaling in the context of muscle hypertrophy.

Genetic alterations in the γ3 isoform do not result in isoform compensation in skeletal muscle from Tg-Prkag3^{225Q} and Prkag3$^{-/-}$ mice (Barnes *et al.*, 2004). However, functional overload could induce a compensation of the other isoforms of the γ subunit. This is may be particularly relevant in the case of the γ1 isoform, which has been found to be expressed in skeletal muscle as a heterotrimeric complex with the α2 and β2 isoforms (Mahlapuu *et al.*, 2004).

5 CONCLUSIONS AND PERSPECTIVES

The aim of this thesis work was to characterize the response of skeletal muscle to various genetic and environmental stressors using different *in vitro* and *in vivo* models. As summarized in Fig. 10, this work provides insight into the mechanisms by which skeletal muscle remodels in response to a variety of stressors.

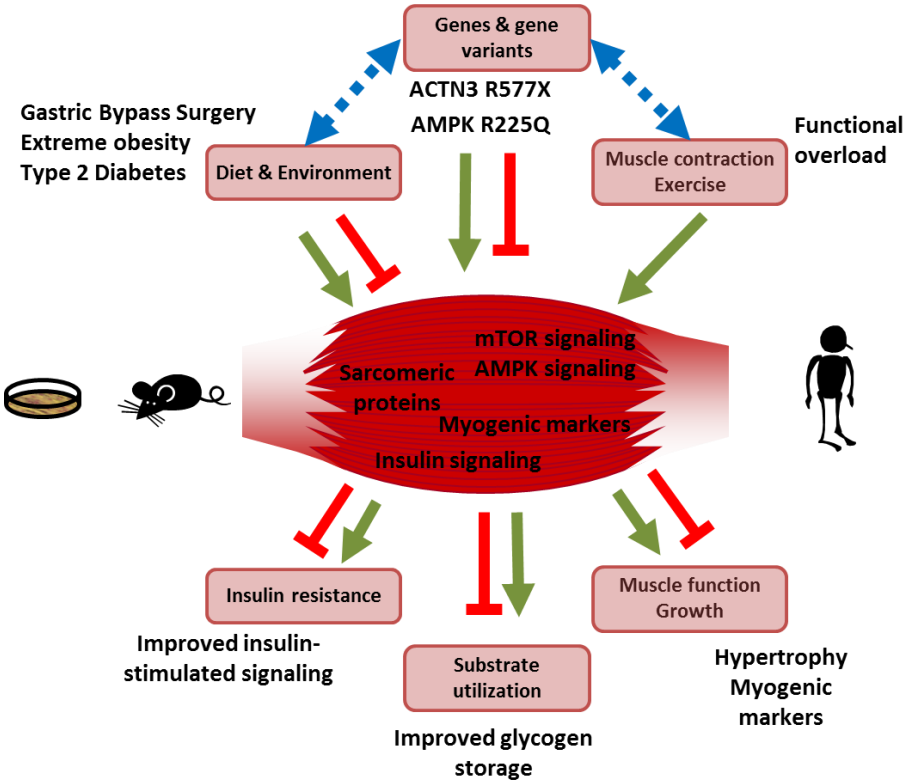

Figure 12: Summary of outcomes of Study I, II, and III.

In **Study I**, an *in vitro* model was established to study local changes in substrate metabolism, insulin action and secreted factors in response to RYGB-induced weight loss, which may secondarily influence whole-body insulin sensitivity. Using human skeletal muscle cell cultures in a unique longitudinal study design provided further insight into mechanisms by which skeletal muscle

is affected by weight-loss surgery. The results generated in this thesis suggest that improvements in glucose disposal in skeletal muscle of extremely obese patients is a reversible defect. A role of the signaling intermediate PRAS40 as a candidate that could regulate the improvements in the metabolism of skeletal muscle following RYGB is also suggested. PRAS40 may very well play a role in improved glucose metabolism following gastric bypass surgery and experiments using small interfering RNA, for example, could allow further insight in this eventual mechanism. Moreover, since PRAS40 is a member of mTORC1, a critical regulator of cell size and growth, an evaluation of whether PRAS40 can potentiate skeletal muscle growth in response to a hypertrophic or atrophic stimuli, in both states of health and disease is warranted. From an ethical point of view, the use of an *in vitro* longitudinal model has additional benefits, since it diminishes the use of animal and human tissues for research purposes. This model also provides an easy, accessible, but still unique approach to dissect intrinsic from systemic factors that influence insulin sensitivity and energy homeostasis.

The resolution of the metabolic disease epidemic largely depends on preventive measures. The use of genetic profiling in the diagnostic and treatment of diseases is an area of molecular medicine in constant evolution. Gaining insight into gene variants modulating disease pathophysiology, as well as metabolic and structural responses to exercise training may direct the development of new, personalized therapeutic tools and interventions, both pharmacological and non-pharmacological. **Study II** addressed the role of the ACTN3 R577X polymorphism in metabolic disease and skeletal muscle hypertrophy, respectively. Since physical exercise is a cornerstone in the prevention and treatment of insulin resistance and T2D, the metabolic oxidative phenotype displayed by ACTN3$^{-/-}$ mice raises a legitimate question towards the beneficial impact of the 577XX genotype in T2D individuals. Although the polymorphism did not seem to be related to clinical parameters measured in this cohort, the genotype distribution was altered between the T2D and both IGT and NGT groups. The vast majority of clinical studies investigating the ACTN3 R577X polymorphism, including **Study II**, have been performed using small size cohorts, which could contribute to type I and II errors. The results generated in this thesis should be replicated

using in larger cohorts. As mentioned previously, given the fact that ACTN3 expression is specific to glycolytic type 2 fibers, the finding that the phenotype observed in ACTN3$^{-/-}$ mice is not entirely copied in humans with the 577XX genotype may be partly attributed to an inter-species difference in skeletal muscle fiber type distribution. To reveal the functional consequences of ACTN3 R577X polymorphism, extreme interventions (run-to-exhaustion, extreme eccentric contraction, high-level athletic performance, immobilization) are often required, suggesting a gene-environment interaction. Future functional studies may highlight whether there is a role between the ACTN3 R577X gene variant and the adaptive response to extreme interventions. Additional studies to elucidate the role of the ACTN3 R577X polymorphism in the adaptive response of skeletal muscle to exercise training would be beneficial to improve personalized exercise intervention in the context of metabolic diseases.

In **Study III**, the role of the AMPK γ3 isoform in skeletal muscle hypertrophy and activation of protein synthesis machinery was evaluated. The results generated in this thesis suggest that the role of AMPK is to favor atrophy rather than to act as a "break" on muscle hypertrophy. This hypothesis could be validated by using other genetically modified mouse models and experimental perturbations such as denervation and tail/hindlimb suspension. Instead of impacting growth as initially hypothesized, the AMPK γ3 isoform may predominantly regulate in glucose and lipid metabolism in skeletal muscle. This suggests that other AMPK isoforms could play a role in the response to hypertrophic or atrophic stimuli. As mentioned earlier, the use of different time-course studies could refine the understanding of the role of AMPK on skeletal muscle growth. Other pathways implicated in skeletal muscle hypertrophy should also be considered, such as phosphatidic acid (You *et al.*, 2014) and focal adhesion kinase (FAK) (Crossland *et al.*, 2013).

Collectively, the results presented in this thesis provide information on the remodeling capacity of skeletal muscle in response to various stressors, including severe weight-loss intervention, gene variants and hypertrophic stimulus. These stressors differently affect skeletal muscle, which adapts via changes in metabolic and growth-related signaling pathways, release of secreted factors such as

cytokines/myokines, as well undergoing changes in structure and substrate utilization. Information provided by this thesis work may one day contribute to improving and optimizing already existing treatments to counter lifestyle-related metabolic diseases.

6 ACKNOWLEDGEMENTS

I would like to thank my main supervisor, Professor **Juleen Zierath**, for allowing me to pursue graduate studies within the group. Thank you for taking me on board and allowing me to mature as an individual and as a scientist. I would also like to express my gratitude to my co-supervisor Dr. **Megan Osler** for the patience and the effort you put into me. I learned a great deal from you and I always felt we were working together as a team.

Thank you, Docent **Alexander Chibalin**. Working with you, especially during my last year with the group, was intellectually stimulating and great fun. You always took time for me and my projects, no matter how very busy you were. Professor **Anna Krook**, I thank you because working and interacting with you was a great pleasure. I highly value your positive attitude and open-door philosophy. Dr. **Marie Björnholm** for being an open-minded and methodical scientist and also for being a caring and empathic person. I value your input about my projects and your generous mentorship. Dr. **Emmani Nascimento**, for mentoring and teaching me, without ever asking anything in return. I learned a great deal from you, thank you. I'm so happy we remain friends. Dr. **Jorge Lira Ruas** and Dr. **Gustavo Nader** for being there and always pouring career- and science-related advice. It is highly appreciated and I hope we keep in touch. Thank you Professor **Erik Näslund** for your collaboration and scientific input in the context of Study I.

Thanks to all the past and present members of the Integrative Physiology group, as well as colleagues from the Department of Physiology and Pharmacology. Dr. **Jorge Correia**, Dr. **Vicente Martínez-Redondo** (and **Kristin**!), and Dr. **Julie Massart** for our beer/hamburger-hunting evenings! I value those nights and secretly hope this little thing will never end. **Rasmus Sjögren** and **Leo Lundell** for your special love (for each other). Dr. **Jonathan Mudry**, for your friendship and a lot of shared memories. Dr. **Ferdinand von Walden**, for all moments and fun and laughs shared together. Dr. **Maxwell Ruby** for our work together on PKN2, your mentoring but most of it, for your friendship. Dr. **Sameer Kulkarni** and Dr. **Robby Tom**. I missed you guys quite a lot after you left. And to YOU, Dr. **Laurène Vetterli**, fantastic person, thank you for an amazing and unique friendship that will last forever.

Many thanks to all the people that made working in the lab special every day. Dr. **Jie Yan**, Dr. **Firoozeh Salehzadeh**, Dr. **Fredirick Mashili**, Dr. **Maria Holmström**, Dr. **Carolina Nylén**, Dr. **Henriette Kirchner**, Dr. **Louise Mannerås Holm**, Dr. **Brendan Egan**, Dr. **Mutsumi Katayama**, Dr. **Boubacar Benziane**, Dr. **Thais de Castro Barbosa**, Dr. **Håkan Karlsson**, Dr. **Lake Jiang**,

Dr. **Hanneke Boon**, Dr. **Melissa Borg**, Dr. **Duarte Ferreira**, Dr. **Sonia Garcia Calzón**, Dr. **Lubna Al-Khalili**, Dr. **Marc Gilbert**. Drs-to-be, labmates, officemates, **David Gray Lassiter**, **Linda Molla**, **Bojana Mićić, Kim Patil**, **Marcus Åhlin**, **Milena Schönke**, **Petter Alm**, **Keith Daniel**, **Chang Liu**, **Manizheh Izadi**, **Leo Agudelo**, **Jenny Lund, Mladen Savić**, I wish you the best ahead, *keep your eyes on the prize*! You guys are great fun and I consider myself lucky to work by your side. Thank you **Tobbe**, **Katrin**, **Eva**, **Ann-Marie**, dear **Margareta Svedlund** and **Arja Kants**. You are pillars in this lab. Thank you to our Animal department, especially to **Melinda**, **Pia** and **Laila**, for your contribution to our work is discrete, but crucial.

I also want to thank my friends from home, my private club from the undergrad years, **Marjorie**, **Evelyne** and **Marie-Ève**, for thinking about me, probably every day, while I was on this journey. Also from back home, many thanks to **Carl**, **Alexia**, **Sab**, **Guillaume**, and **Amélie**, for your encouragements. They made a difference. Dear **Maria Rita**, **Paolo**, **Véro**, **Fabien** and **Marylou**, I really, really hope we get together again soon, preferably in the south of Italy, and I thank you for caring and cheering.

Thank you also to my dear friends from pretty Stockholm for being a part of this almost-five year journey. For early mornings at the pool, early (sometimes late) hours on the bike in Erstaviken, summer swims in Sickla, everyday ramblings and so, so much more! **Romain** and **Anna**, **Pavel**, **Eugenia**, **Ester**, **Joan**, **Daniel**, **Susi**, **Peio, Nico, Jenny**. To my crossfit home, dear **Camilla** (you are a truly inspiring person!), **Calvin**, **Kristina** and **Leo**, thank you for always welcoming me and putting work off my mind with burpees and overhead squats. I just love every minute I spend at the gym. **Erik**, **Susi**, **Pim**, **Helena**, **Anna M**., for you guys are always great fun and I'm glad of the rides we had. **Tomas**, a unique friend you are, merci! **Nils**, fantastic housemate, what great company you were back in the days in Årsta. **Haydée**, thank you for putting a roof over my head for more than two years, for your trust, and your friendship. **Loes**, **Audrey**, **Claudia**, and Dr. **Anne van Der Does**, great friends I met here, but are now living somewhere else… where I can visit them!

Finally, my main thanks, to my parents, **Céline** and **Bernard Riedl**, for unconditional love and support. Throughout this journey, you ALWAYS believed in me and encouraged me like no one else. My brother **Johann**, for being always a great supportive fellow and comrade. I miss you. My sister **Catherine**, for never giving up. The rest of my family, **Marc**, **Michel**, **Anne**, **Bob**, **Danielle** and **Diane** for sticking up with me in your own way.

7 REFERENCES

Adams TD, Gress RE, Smith SC, Halverson RC, Simper SC, Rosamond WD, Lamonte MJ, Stroup AM & Hunt SC. (2007). Long-term mortality after gastric bypass surgery. *N Engl J Med* **357,** 753-761.

Agbulut O, Noirez P, Beaumont F & Butler-Browne G. (2003). Myosin heavy chain isoforms in postnatal muscle development of mice. *Biol Cell* **95,** 399-406.

Aguirre V, Uchida T, Yenush L, Davis R & White MF. (2000). The c-Jun NH(2)-terminal kinase promotes insulin resistance during association with insulin receptor substrate-1 and phosphorylation of Ser(307). *J Biol Chem* **275,** 9047-9054.

Al-Khalili L, Chibalin AV, Kannisto K, Zhang BB, Permert J, Holman GD, Ehrenborg E, Ding VD, Zierath JR & Krook A. (2003). Insulin action in cultured human skeletal muscle cells during differentiation: assessment of cell surface GLUT4 and GLUT1 content. *Cell Mol Life Sci* **60,** 991-998.

Arimura C, Suzuki T, Yanagisawa M, Imamura M, Hamada Y & Masaki T. (1988). Primary structure of chicken skeletal muscle and fibroblast alpha-actinins deduced from cDNA sequences. *Eur J Biochem* **177,** 649-655.

Ashwell M, Gunn P & Gibson S. (2012). Waist-to-height ratio is a better screening tool than waist circumference and BMI for adult cardiometabolic risk factors: systematic review and meta-analysis. *Obes Rev* **13,** 275-286.

Baldwin KM, Valdez V, Schrader LF & Herrick RE. (1981). Effect of functional overload on substrate oxidation capacity of skeletal muscle. *J Appl Physiol Respir Environ Exerc Physiol* **50,** 1272-1276.

Barany M. (1967). ATPase activity of myosin correlated with speed of muscle shortening. *J Gen Physiol* **50,** Suppl:197-218.

Barnes BR, Glund S, Long YC, Hjalm G, Andersson L & Zierath JR. (2005a). 5'-AMP-activated protein kinase regulates skeletal muscle glycogen content and ergogenics. *FASEB J* **19,** 773-779.

Barnes BR, Long YC, Steiler TL, Leng Y, Galuska D, Wojtaszewski JF, Andersson L & Zierath JR. (2005b). Changes in exercise-induced gene

expression in 5'-AMP-activated protein kinase gamma3-null and gamma3 R225Q transgenic mice. *Diabetes* **54,** 3484-3489.

Barnes BR, Marklund S, Steiler TL, Walter M, Hjalm G, Amarger V, Mahlapuu M, Leng Y, Johansson C, Galuska D, Lindgren K, Abrink M, Stapleton D, Zierath JR & Andersson L. (2004). The 5'-AMP-activated protein kinase gamma3 isoform has a key role in carbohydrate and lipid metabolism in glycolytic skeletal muscle. *J Biol Chem* **279,** 38441-38447.

Barrès R, Kirchner H, Rasmussen M, Yan J, Kantor FR, Krook A, Näslund E & Zierath JR. (2013). Weight loss after gastric bypass surgery in human obesity remodels promoter methylation. *Cell Rep* **3,** 1020-1027.

Battaglia GM, Zheng D, Hickner RC & Houmard JA. (2012). Effect of exercise training on metabolic flexibility in response to a high-fat diet in obese individuals. *Am J Physiol Endocrinol Metab* **303,** E1440-1445.

Beggs AH, Byers TJ, Knoll JH, Boyce FM, Bruns GA & Kunkel LM. (1992). Cloning and characterization of two human skeletal muscle alpha-actinin genes located on chromosomes 1 and 11. *J Biol Chem* **267,** 9281-9288.

Bellacosa A, Chan TO, Ahmed NN, Datta K, Malstrom S, Stokoe D, McCormick F, Feng J & Tsichlis P. (1998). Akt activation by growth factors is a multiple-step process: the role of the PH domain. *Oncogene* **17,** 313-325.

Bentzinger CF, Wang YX & Rudnicki MA. (2012). Building muscle: molecular regulation of myogenesis. *Cold Spring Harb Perspect Biol* **4**.

Bergstrom J & Hultman E. (1966). Muscle glycogen synthesis after exercise: an enhancing factor localized to the muscle cells in man. *Nature* **210,** 309-310.

Berman Y & North KN. (2010). A gene for speed: the emerging role of alpha-actinin-3 in muscle metabolism. *Physiology (Bethesda)* **25,** 250-259.

Bikman BT, Zheng D, Pories WJ, Chapman W, Pender JR, Bowden RC, Reed MA, Cortright RN, Tapscott EB, Houmard JA, Tanner CJ, Lee J & Dohm GL. (2008). Mechanism for improved insulin sensitivity after gastric bypass surgery. *J Clin Endocrinol Metab* **93,** 4656-4663.

Bodine SC & Baar K. (2012). Analysis of skeletal muscle hypertrophy in models of increased loading. *Methods Mol Biol* **798,** 213-229.

Bodine SC, Stitt TN, Gonzalez M, Kline WO, Stover GL, Bauerlein R, Zlotchenko E, Scrimgeour A, Lawrence JC, Glass DJ & Yancopoulos GD. (2001). Akt/mTOR pathway is a crucial regulator of skeletal muscle hypertrophy and can prevent muscle atrophy in vivo. *Nat Cell Biol* **3,** 1014-1019.

Bolster DR, Crozier SJ, Kimball SR & Jefferson LS. (2002). AMP-activated protein kinase suppresses protein synthesis in rat skeletal muscle through down-regulated mammalian target of rapamycin (mTOR) signaling. *J Biol Chem* **277,** 23977-23980.

Bonnefond A, Froguel P & Vaxillaire M. (2010). The emerging genetics of type 2 diabetes. *Trends Mol Med* **16,** 407-416.

Bouchard C, An P, Rice T, Skinner JS, Wilmore JH, Gagnon J, Perusse L, Leon AS & Rao DC. (1999). Familial aggregation of VO(2max) response to exercise training: results from the HERITAGE Family Study. *J Appl Physiol (1985)* **87,** 1003-1008.

Bouchard C, Daw EW, Rice T, Perusse L, Gagnon J, Province MA, Leon AS, Rao DC, Skinner JS & Wilmore JH. (1998). Familial resemblance for VO2max in the sedentary state: the HERITAGE family study. *Med Sci Sports Exerc* **30,** 252-258.

Bouchard C, Sarzynski MA, Rice TK, Kraus WE, Church TS, Sung YJ, Rao DC & Rankinen T. (2011). Genomic predictors of the maximal O(2) uptake response to standardized exercise training programs. *J Appl Physiol (1985)* **110,** 1160-1170.

Boule NG, Haddad E, Kenny GP, Wells GA & Sigal RJ. (2001). Effects of exercise on glycemic control and body mass in type 2 diabetes mellitus: a meta-analysis of controlled clinical trials. *JAMA* **286,** 1218-1227.

Boyle KE, Zheng D, Anderson EJ, Neufer PD & Houmard JA. (2012). Mitochondrial lipid oxidation is impaired in cultured myotubes from obese humans. *Int J Obes (Lond)* **36,** 1025-1031.

Brooks GA & Mercier J. (1994) Balance of carbohydrate and lipid utilization during exercise: the "crossover" concept. *J Appl Physiol (1985)* **76,** 2253-2261.

Broos S, Malisoux L, Theisen D, Francaux M, Deldicque L & Thomis MA. (2012). Role of alpha-actinin-3 in contractile properties of human single muscle fibers: a case series study in paraplegics. *PLoS One* **7,** e49281.

Buchwald H, Avidor Y, Braunwald E, Jensen MD, Pories W, Fahrbach K & Schoelles K. (2004). Bariatric surgery: a systematic review and meta-analysis. *JAMA* **292,** 1724-1737.

Buchwald H, Buchwald JN & McGlennon TW. (2014). Systematic review and meta-analysis of medium-term outcomes after banded Roux-en-Y gastric bypass. *Obes Surg* **24,** 1536-1551.

Buchwald H & Oien DM. (2009). Metabolic/bariatric surgery Worldwide 2008. *Obes Surg* **19,** 1605-1611.

Buller AJ, Eccles JC & Eccles RM. (1960). Differentiation of fast and slow muscles in the cat hind limb. *J Physiol* **150,** 399-416.

Carlsson LM, Peltonen M, Ahlin S, Anveden A, Bouchard C, Carlsson B, Jacobson P, Lonroth H, Maglio C, Naslund I, Pirazzi C, Romeo S, Sjoholm K, Sjostrom E, Wedel H, Svensson PA & Sjostrom L. (2012). Bariatric surgery and prevention of type 2 diabetes in Swedish obese subjects. *N Engl J Med* **367,** 695-704.

Chabowski A, Chatham JC, Tandon NN, Calles-Escandon J, Glatz JF, Luiken JJ & Bonen A. (2006). Fatty acid transport and FAT/CD36 are increased in red but not in white skeletal muscle of ZDF rats. *Am J Physiol Endocrinol Metab* **291,** E675-682.

Colberg SR, Sigal RJ, Fernhall B, Regensteiner JG, Blissmer BJ, Rubin RR, Chasan-Taber L, Albright AL & Braun B. (2010). Exercise and type 2 diabetes: the American College of Sports Medicine and the American Diabetes Association: joint position statement. *Diabetes Care* **33,** e147-167.

Costford SR, Kavaslar N, Ahituv N, Chaudhry SN, Schackwitz WS, Dent R, Pennacchio LA, McPherson R & Harper ME. (2007). Gain-of-function R225W mutation in human AMPKgamma(3) causing increased glycogen and decreased triglyceride in skeletal muscle. *PLoS One* **2,** e903.

Crossland H, Kazi AA, Lang CH, Timmons JA, Pierre P, Wilkinson DJ, Smith K, Szewczyk NJ & Atherton PJ. (2013). Focal adhesion kinase is required for IGF-I-mediated growth of skeletal muscle cells via a TSC2/mTOR/S6K1-associated pathway. *Am J Physiol Endocrinol Metab* **305,** E183-193.

Danaei G, Finucane MM, Lu Y, Singh GM, Cowan MJ, Paciorek CJ, Lin JK, Farzadfar F, Khang YH, Stevens GA, Rao M, Ali MK, Riley LM,

Robinson CA & Ezzati M. (2011). National, regional, and global trends in fasting plasma glucose and diabetes prevalence since 1980: systematic analysis of health examination surveys and epidemiological studies with 370 country-years and 2.7 million participants. *Lancet* **378,** 31-40.

Danser AH, Schalekamp MA, Bax WA, van den Brink AM, Saxena PR, Riegger GA & Schunkert H. (1995). Angiotensin-converting enzyme in the human heart. Effect of the deletion/insertion polymorphism. *Circulation* **92,** 1387-1388.

Davies SP, Helps NR, Cohen PT & Hardie DG. (1995). 5'-AMP inhibits dephosphorylation, as well as promoting phosphorylation, of the AMP-activated protein kinase. Studies using bacterially expressed human protein phosphatase-2C alpha and native bovine protein phosphatase-2AC. *FEBS Lett* **377,** 421-425.

De Moor MH, Spector TD, Cherkas LF, Falchi M, Hottenga JJ, Boomsma DI & De Geus EJ. (2007). Genome-wide linkage scan for athlete status in 700 British female DZ twin pairs. *Twin Res Hum Genet* **10,** 812-820.

DeFronzo RA, Jacot E, Jequier E, Maeder E, Wahren J & Felber JP. (1981). The effect of insulin on the disposal of intravenous glucose. Results from indirect calorimetry and hepatic and femoral venous catheterization. *Diabetes* **30,** 1000-1007.

Delin CR, Watts JM, Saebel JL & Anderson PG. (1997). Eating behavior and the experience of hunger following gastric bypass surgery for morbid obesity. *Obes Surg* **7,** 405-413.

DeNardi C, Ausoni S, Moretti P, Gorza L, Velleca M, Buckingham M & Schiaffino S. (1993). Type 2X-myosin heavy chain is coded by a muscle fiber type-specific and developmentally regulated gene. *J Cell Biol* **123,** 823-835.

Dietrichson P, Coakley J, Smith PE, Griffiths RD, Helliwell TR & Edwards RH. (1987). Conchotome and needle percutaneous biopsy of skeletal muscle. *J Neurol Neurosurg Psychiatry* **50,** 1461-1467.

Dimas AS, Lagou V, Barker A, Knowles JW, Magi R, Hivert MF, Benazzo A, Rybin D, Jackson AU, Stringham HM, Song C, Fischer-Rosinsky A, Boesgaard TW, Grarup N, Abbasi FA, Assimes TL, Hao K, Yang X, Lecoeur C, Barroso I, Bonnycastle LL, Bottcher Y, Bumpstead S, Chines PS, Erdos MR, Graessler J, Kovacs P, Morken MA, Narisu N, Payne F, Stancakova A, Swift AJ, Tonjes A, Bornstein SR, Cauchi S, Froguel P,

Meyre D, Schwarz PE, Haring HU, Smith U, Boehnke M, Bergman RN, Collins FS, Mohlke KL, Tuomilehto J, Quertemous T, Lind L, Hansen T, Pedersen O, Walker M, Pfeiffer AF, Spranger J, Stumvoll M, Meigs JB, Wareham NJ, Kuusisto J, Laakso M, Langenberg C, Dupuis J, Watanabe RM, Florez JC, Ingelsson E, McCarthy MI & Prokopenko I. (2014). Impact of type 2 diabetes susceptibility variants on quantitative glycemic traits reveals mechanistic heterogeneity. *Diabetes* **63,** 2158-2171.

Dirksen C, Jorgensen NB, Bojsen-Moller KN, Jacobsen SH, Hansen DL, Worm D, Holst JJ & Madsbad S. (2012). Mechanisms of improved glycaemic control after Roux-en-Y gastric bypass. *Diabetologia* **55,** 1890-1901.

Druzhevskaya AM, Ahmetov, II, Astratenkova IV & Rogozkin VA. (2008). Association of the ACTN3 R577X polymorphism with power athlete status in Russians. *Eur J Appl Physiol* **103,** 631-634.

Ebashi S & Ebashi F. (1965). Alpha-actinin, a new structural protein from striated muscle. I. Preparation and action on actomyosinatp interaction. *J Biochem* **58,** 7-12.

Egan B & Zierath JR. (2013). Exercise metabolism and the molecular regulation of skeletal muscle adaptation. *Cell Metab* **17,** 162-184.

Egerman MA & Glass DJ. (2014). Signaling pathways controlling skeletal muscle mass. *Crit Rev Biochem Mol Biol* **49,** 59-68.

Emanuelli B, Peraldi P, Filloux C, Sawka-Verhelle D, Hilton D & Van Obberghen E. (2000). SOCS-3 is an insulin-induced negative regulator of insulin signaling. *J Biol Chem* **275,** 15985-15991.

Eynon N, Duarte JA, Oliveira J, Sagiv M, Yamin C, Meckel Y & Goldhammer E. (2009). ACTN3 R577X polymorphism and Israeli top-level athletes. *Int J Sports Med* **30,** 695-698.

Eynon N, Hanson ED, Lucia A, Houweling PJ, Garton F, North KN & Bishop DJ. (2013). Genes for elite power and sprint performance: ACTN3 leads the way. *Sports Med* **43,** 803-817.

Ferrannini E & Mingrone G. (2009). Impact of different bariatric surgical procedures on insulin action and beta-cell function in type 2 diabetes. *Diabetes Care* **32,** 514-520.

Friedman JE, Dohm GL, Leggett-Frazier N, Elton CW, Tapscott EB, Pories WP & Caro JF. (1992). Restoration of insulin responsiveness in skeletal muscle of morbidly obese patients after weight loss. Effect on muscle

glucose transport and glucose transporter GLUT4. *J Clin Invest* **89,** 701-705.

Fritz T, Caidahl K, Osler M, Ostenson CG, Zierath JR & Wandell P. (2011). Effects of Nordic walking on healthrelated quality of life in overweight individuals with type 2 diabetes mellitus, impaired or normal glucose tolerance. *Diabet Med* **28,** 1362-1372.

Fritz T, Caidahl K, Krook A, Lundstrom P, Mashili F, Osler M, Szekeres FL, Östenson CG, Wändell P & Zierath JR. (2013). Effects of Nordic walking on cardiovascular risk factors in overweight individuals with type 2 diabetes, impaired or normal glucose tolerance. *Diabetes Metab Res Rev* **29,** 25-32.

Gaitanos GC, Williams C, Boobis LH & Brooks S. (1993). Human muscle metabolism during intermittent maximal exercise. *J Appl Physiol (1985)* **75,** 712-719.

Gallagher D, Belmonte D, Deurenberg P, Wang Z, Krasnow N, Pi-Sunyer FX & Heymsfield SB. (1998). Organ-tissue mass measurement allows modeling of REE and metabolically active tissue mass. *Am J Physiol* **275,** E249-258.

Garcia-Roves PM, Osler ME, Holmstrom MH & Zierath JR. (2008). Gain-of-function R225Q mutation in AMP-activated protein kinase gamma3 subunit increases mitochondrial biogenesis in glycolytic skeletal muscle. *J Biol Chem* **283,** 35724-35734.

Garton FC, Seto JT, Quinlan KG, Yang N, Houweling PJ & North KN. (2014). alpha-Actinin-3 deficiency alters muscle adaptation in response to denervation and immobilization. *Hum Mol Genet* **23,** 1879-1893.

Goodpaster BH, Delany JP, Otto AD, Kuller L, Vockley J, South-Paul JE, Thomas SB, Brown J, McTigue K, Hames KC, Lang W & Jakicic JM. (2010). Effects of diet and physical activity interventions on weight loss and cardiometabolic risk factors in severely obese adults: a randomized trial. *JAMA* **304,** 1795-1802.

Goodyear LJ, Hirshman MF, Smith RJ & Horton ES. (1991). Glucose transporter number, activity, and isoform content in plasma membranes of red and white skeletal muscle. *Am J Physiol* **261,** E556-561.

Greenhaff PL, Soderlund K, Ren JM & Hultman E. (1993). Energy metabolism in single human muscle fibres during intermittent contraction with occluded circulation. *J Physiol* **460,** 443-453.

Gual P, Le Marchand-Brustel Y & Tanti JF. (2005). Positive and negative regulation of insulin signaling through IRS-1 phosphorylation. *Biochimie* **87,** 99-109.

Guesbeck NR, Hickey MS, MacDonald KG, Pories WJ, Harper I, Ravussin E, Dohm GL & Houmard JA. (2001). Substrate utilization during exercise in formerly morbidly obese women. *J Appl Physiol (1985)* **90,** 1007-1012.

Gwinn DM, Shackelford DB, Egan DF, Mihaylova MM, Mery A, Vasquez DS, Turk BE & Shaw RJ. (2008). AMPK phosphorylation of raptor mediates a metabolic checkpoint. *Mol Cell* **30,** 214-226.

Hardie DG. (2014). AMPK--sensing energy while talking to other signaling pathways. *Cell Metab* **20,** 939-952.

Hawley JA & Gibala MJ. (2012). What's new since Hippocrates? Preventing type 2 diabetes by physical exercise and diet. *Diabetologia* **55,** 535-539.

Hawley SA, Davison M, Woods A, Davies SP, Beri RK, Carling D & Hardie DG. (1996). Characterization of the AMP-activated protein kinase kinase from rat liver and identification of threonine 172 as the major site at which it phosphorylates AMP-activated protein kinase. *J Biol Chem* **271,** 27879-27887.

He C, Bassik MC, Moresi V, Sun K, Wei Y, Zou Z, An Z, Loh J, Fisher J, Sun Q, Korsmeyer S, Packer M, May HI, Hill JA, Virgin HW, Gilpin C, Xiao G, Bassel-Duby R, Scherer PE & Levine B. (2012). Exercise-induced BCL2-regulated autophagy is required for muscle glucose homeostasis. *Nature* **481,** 511-515.

Holland WL, Bikman BT, Wang LP, Yuguang G, Sargent KM, Bulchand S, Knotts TA, Shui G, Clegg DJ, Wenk MR, Pagliassotti MJ, Scherer PE & Summers SA. (2011). Lipid-induced insulin resistance mediated by the proinflammatory receptor TLR4 requires saturated fatty acid-induced ceramide biosynthesis in mice. *J Clin Invest* **121,** 1858-1870.

Hubbard SR, Wei L, Ellis L & Hendrickson WA. (1994). Crystal structure of the tyrosine kinase domain of the human insulin receptor. *Nature* **372,** 746-754.

Huxley AF & Niedergerke R. (1954). Structural changes in muscle during contraction; interference microscopy of living muscle fibres. *Nature* **173,** 971-973.

Huxley H & Hanson J. (1954). Changes in the cross-striations of muscle during contraction and stretch and their structural interpretation. *Nature* **173,** 973-976.

IDF. (2006). Definition and diagnosis of diabetes mellitus and intermediate hyperglycemia.

Im SH & Rao A. (2004). Activation and deactivation of gene expression by Ca2+/calcineurin-NFAT-mediated signaling. *Mol Cells* **18,** 1-9.

Imayama I, Ulrich CM, Alfano CM, Wang C, Xiao L, Wener MH, Campbell KL, Duggan C, Foster-Schubert KE, Kong A, Mason CE, Wang CY, Blackburn GL, Bain CE, Thompson HJ & McTiernan A. (2012). Effects of a caloric restriction weight loss diet and exercise on inflammatory biomarkers in overweight/obese postmenopausal women: a randomized controlled trial. *Cancer Res* **72,** 2314-2326.

Inoki K, Li Y, Zhu T, Wu J & Guan KL. (2002). TSC2 is phosphorylated and inhibited by Akt and suppresses mTOR signalling. *Nat Cell Biol* **4,** 648-657.

Inoki K, Zhu T & Guan KL. (2003). TSC2 mediates cellular energy response to control cell growth and survival. *Cell* **115,** 577-590.

Itani SI, Ruderman NB, Schmieder F & Boden G. (2002). Lipid-induced insulin resistance in human muscle is associated with changes in diacylglycerol, protein kinase C, and IkappaB-alpha. *Diabetes* **51,** 2005-2011.

Izumi T, White MF, Kadowaki T, Takaku F, Akanuma Y & Kasuga M. (1987). Insulin-like growth factor I rapidly stimulates tyrosine phosphorylation of a Mr 185,000 protein in intact cells. *J Biol Chem* **262,** 1282-1287.

Kim J, Kundu M, Viollet B & Guan KL. (2011). AMPK and mTOR regulate autophagy through direct phosphorylation of Ulk1. *Nat Cell Biol* **13,** 132-141.

Kjobsted R, Treebak JT, Fentz J, Lantier L, Viollet B, Birk JB, Schjerling P, Bjornholm M, Zierath JR & Wojtaszewski JF. (2014). Prior AICAR stimulation increases insulin sensitivity in mouse skeletal muscle in an AMPK-dependent manner. *Diabetes*.

Klein DK, Pilegaard H, Treebak JT, Jensen TE, Viollet B, Schjerling P & Wojtaszewski JF. (2007). Lack of AMPKalpha2 enhances pyruvate dehydrogenase activity during exercise. *Am J Physiol Endocrinol Metab* **293,** E1242-1249.

Knowler WC, Barrett-Connor E, Fowler SE, Hamman RF, Lachin JM, Walker EA & Nathan DM. (2002). Reduction in the incidence of type 2 diabetes with lifestyle intervention or metformin. *N Engl J Med* **346,** 393-403.

Krssak M, Falk Petersen K, Dresner A, DiPietro L, Vogel SM, Rothman DL, Roden M & Shulman GI. (1999). Intramyocellular lipid concentrations are correlated with insulin sensitivity in humans: a 1H NMR spectroscopy study. *Diabetologia* **42,** 113-116.

Labeit S, Gibson T, Lakey A, Leonard K, Zeviani M, Knight P, Wardale J & Trinick J. (1991). Evidence that nebulin is a protein-ruler in muscle thin filaments. *FEBS Lett* **282,** 313-316.

Labeit S & Kolmerer B. (1995). Titins: giant proteins in charge of muscle ultrastructure and elasticity. *Science* **270,** 293-296.

Larsen S, Stride N, Hey-Mogensen M, Hansen CN, Andersen JL, Madsbad S, Worm D, Helge JW & Dela F. (2011). Increased mitochondrial substrate sensitivity in skeletal muscle of patients with type 2 diabetes. *Diabetologia* **54,** 1427-1436.

Larsson L, Edstrom L, Lindegren B, Gorza L & Schiaffino S. (1991). MHC composition and enzyme-histochemical and physiological properties of a novel fast-twitch motor unit type. *Am J Physiol* **261,** C93-101.

Latres E, Amini AR, Amini AA, Griffiths J, Martin FJ, Wei Y, Lin HC, Yancopoulos GD & Glass DJ. (2005). Insulin-like growth factor-1 (IGF-1) inversely regulates atrophy-induced genes via the phosphatidylinositol 3-kinase/Akt/mammalian target of rapamycin (PI3K/Akt/mTOR) pathway. *J Biol Chem* **280,** 2737-2744.

Lee AD, Hansen PA & Holloszy JO. (1995). Wortmannin inhibits insulin-stimulated but not contraction-stimulated glucose transport activity in skeletal muscle. *FEBS Lett* **361,** 51-54.

Lewis CM & Knight J. (2012). Introduction to genetic association studies. *Cold Spring Harb Protoc* **2012,** 297-306.

Lucia A, Gomez-Gallego F, Santiago C, Perez M, Mate-Munoz JL, Chamorro-Vina C, Nogales-Gadea G, Foster C, Rubio JC, Andreu AL, Martin MA

& Arenas J. (2007). The 577X allele of the ACTN3 gene is associated with improved exercise capacity in women with McArdle's disease. *Neuromuscul Disord* **17,** 603-610.

Lund S, Holman GD, Schmitz O & Pedersen O. (1995). Contraction stimulates translocation of glucose transporter GLUT4 in skeletal muscle through a mechanism distinct from that of insulin. *Proc Natl Acad Sci U S A* **92,** 5817-5821.

Lundberg TR, Fernandez-Gonzalo R, Norrbom J, Fischer H, Tesch PA & Gustafsson T. (2014). Truncated splice variant PGC-1alpha4 is not associated with exercise-induced human muscle hypertrophy. *Acta Physiol (Oxf)* **212,** 142-151.

MacArthur DG, Seto JT, Chan S, Quinlan KG, Raftery JM, Turner N, Nicholson MD, Kee AJ, Hardeman EC, Gunning PW, Cooney GJ, Head SI, Yang N & North KN. (2008). An Actn3 knockout mouse provides mechanistic insights into the association between alpha-actinin-3 deficiency and human athletic performance. *Hum Mol Genet* **17,** 1076-1086.

MacArthur DG, Seto JT, Raftery JM, Quinlan KG, Huttley GA, Hook JW, Lemckert FA, Kee AJ, Edwards MR, Berman Y, Hardeman EC, Gunning PW, Easteal S, Yang N & North KN. (2007). Loss of ACTN3 gene function alters mouse muscle metabolism and shows evidence of positive selection in humans. *Nat Genet* **39,** 1261-1265.

Madsbad S, Dirksen C & Holst JJ. (2014). Mechanisms of changes in glucose metabolism and bodyweight after bariatric surgery. *Lancet Diabetes Endocrinol* **2,** 152-164.

Mahlapuu M, Johansson C, Lindgren K, Hjalm G, Barnes BR, Krook A, Zierath JR, Andersson L & Marklund S. (2004). Expression profiling of the gamma-subunit isoforms of AMP-activated protein kinase suggests a major role for gamma3 in white skeletal muscle. *Am J Physiol Endocrinol Metab* **286,** E194-200.

Masaki T, Endo M & Ebashi S. (1967). Localization of 6S component of a alpha-actinin at Z-band. *J Biochem* **62,** 630-632.

Mashili F, Chibalin AV, Krook A & Zierath JR. (2013). Constitutive STAT3 phosphorylation contributes to skeletal muscle insulin resistance in type 2 diabetes. *Diabetes* **62,** 457-465.

McCullagh KJ, Calabria E, Pallafacchina G, Ciciliot S, Serrano AL, Argentini C, Kalhovde JM, Lomo T & Schiaffino S. (2004). NFAT is a nerve activity sensor in skeletal muscle and controls activity-dependent myosin switching. *Proc Natl Acad Sci U S A* **101,** 10590-10595.

McGee SL, Mustard KJ, Hardie DG & Baar K. (2008). Normal hypertrophy accompanied by phosphoryation and activation of AMP-activated protein kinase alpha1 following overload in LKB1 knockout mice. *J Physiol* **586,** 1731-1741.

McPherron AC, Lawler AM & Lee SJ. (1997). Regulation of skeletal muscle mass in mice by a new TGF-beta superfamily member. *Nature* **387,** 83-90.

Mikines KJ, Sonne B, Farrell PA, Tronier B & Galbo H. (1988). Effect of physical exercise on sensitivity and responsiveness to insulin in humans. *Am J Physiol* **254,** E248-259.

Milan D, Jeon JT, Looft C, Amarger V, Robic A, Thelander M, Rogel-Gaillard C, Paul S, Iannuccelli N, Rask L, Ronne H, Lundstrom K, Reinsch N, Gellin J, Kalm E, Roy PL, Chardon P & Andersson L. (2000). A mutation in PRKAG3 associated with excess glycogen content in pig skeletal muscle. *Science* **288,** 1248-1251.

Mills M, Yang N, Weinberger R, Vander Woude DL, Beggs AH, Easteal S & North K. (2001). Differential expression of the actin-binding proteins, alpha-actinin-2 and -3, in different species: implications for the evolution of functional redundancy. *Hum Mol Genet* **10,** 1335-1346.

Moller DE & Kaufman KD. (2005). Metabolic syndrome: a clinical and molecular perspective. *Annu Rev Med* **56,** 45-62.

Mounier R, Lantier L, Leclerc J, Sotiropoulos A, Foretz M & Viollet B. (2011). Antagonistic control of muscle cell size by AMPK and mTORC1. *Cell Cycle* **10,** 2640-2646.

Mounier R, Lantier L, Leclerc J, Sotiropoulos A, Pende M, Daegelen D, Sakamoto K, Foretz M & Viollet B. (2009). Important role for AMPKalpha1 in limiting skeletal muscle cell hypertrophy. *FASEB J* **23,** 2264-2273.

Needham DM. (1926). Red and white muscle. *Physiol Rev* **6,** 1-27.

Nesher R, Karl IE & Kipnis DM. (1985). Dissociation of effects of insulin and contraction on glucose transport in rat epitrochlearis muscle. *Am J Physiol* **249,** C226-232.

Niemi AK & Majamaa K. (2005). Mitochondrial DNA and ACTN3 genotypes in Finnish elite endurance and sprint athletes. *Eur J Hum Genet* **13,** 965-969.

Norman B, Esbjornsson M, Rundqvist H, Osterlund T, Glenmark B & Jansson E. (2014). ACTN3 genotype and modulation of skeletal muscle response to exercise in human subjects. *J Appl Physiol (1985)* **116,** 1197-1203.

Norman B, Esbjornsson M, Rundqvist H, Osterlund T, von Walden F & Tesch PA. (2009). Strength, power, fiber types, and mRNA expression in trained men and women with different ACTN3 R577X genotypes. *J Appl Physiol* **106,** 959-965.

North KN & Beggs AH. (1996). Deficiency of a skeletal muscle isoform of alpha-actinin (alpha-actinin-3) in merosin-positive congenital muscular dystrophy. *Neuromuscul Disord* **6,** 229-235.

North KN, Yang N, Wattanasirichaigoon D, Mills M, Easteal S & Beggs AH. (1999). A common nonsense mutation results in alpha-actinin-3 deficiency in the general population. *Nat Genet* **21,** 353-354.

Oberbach A, Bossenz Y, Lehmann S, Niebauer J, Adams V, Paschke R, Schon MR, Bluher M & Punkt K. (2006). Altered fiber distribution and fiber-specific glycolytic and oxidative enzyme activity in skeletal muscle of patients with type 2 diabetes. *Diabetes Care* **29,** 895-900.

Olsson KE & Saltin B. (1970). Variation in total body water with muscle glycogen changes in man. *Acta Physiol Scand* **80,** 11-18.

Papadimitriou ID, Papadopoulos C, Kouvatsi A & Triantaphyllidis C. (2008). The ACTN3 gene in elite Greek track and field athletes. *Int J Sports Med* **29,** 352-355.

Pellegrino MA, Canepari M, Rossi R, D'Antona G, Reggiani C & Bottinelli R. (2003). Orthologous myosin isoforms and scaling of shortening velocity with body size in mouse, rat, rabbit and human muscles. *J Physiol* **546,** 677-689.

Perez-Schindler J, Summermatter S, Santos G, Zorzato F & Handschin C. (2013). The transcriptional coactivator PGC-1alpha is dispensable for

chronic overload-induced skeletal muscle hypertrophy and metabolic remodeling. *Proc Natl Acad Sci U S A* **110,** 20314-20319.

Pillon NJ, Bilan PJ, Fink LN & Klip A. (2013). Cross-talk between skeletal muscle and immune cells: muscle-derived mediators and metabolic implications. *Am J Physiol Endocrinol Metab* **304,** E453-465.

Plecka Ostlund M, Marsk R, Rasmussen F, Lagergren J & Naslund E. (2011). Morbidity and mortality before and after bariatric surgery for morbid obesity compared with the general population. *Br J Surg* **98,** 811-816.

Podolsky RJ & Schoenberg M. (1983). Force generation and shortening in skeletal muscle. In *Handbook of Physiology, Skeletal Muscle,* pp. 173-188.

Quinlan KG, Seto JT, Turner N, Vandebrouck A, Floetenmeyer M, Macarthur DG, Raftery JM, Lek M, Yang N, Parton RG, Cooney GJ & North KN. (2010). Alpha-actinin-3 deficiency results in reduced glycogen phosphorylase activity and altered calcium handling in skeletal muscle. *Hum Mol Genet* **19,** 1335-1346.

Ribeiro Ede A, Jr., Pinotsis N, Ghisleni A, Salmazo A, Konarev PV, Kostan J, Sjoblom B, Schreiner C, Polyansky AA, Gkougkoulia EA, Holt MR, Aachmann FL, Zagrovic B, Bordignon E, Pirker KF, Svergun DI, Gautel M & Djinovic-Carugo K. (2014). The structure and regulation of human muscle alpha-actinin. *Cell* **159,** 1447-1460.

Rieusset J, Bouzakri K, Chevillotte E, Ricard N, Jacquet D, Bastard JP, Laville M & Vidal H. (2004). Suppressor of cytokine signaling 3 expression and insulin resistance in skeletal muscle of obese and type 2 diabetic patients. *Diabetes* **53,** 2232-2241.

Rigat B, Hubert C, Alhenc-Gelas F, Cambien F, Corvol P & Soubrier F. (1990). An insertion/deletion polymorphism in the angiotensin I-converting enzyme gene accounting for half the variance of serum enzyme levels. *J Clin Invest* **86,** 1343-1346.

Roth SM, Walsh S, Liu D, Metter EJ, Ferrucci L & Hurley BF. (2008). The ACTN3 R577X nonsense allele is under-represented in elite-level strength athletes. *Eur J Hum Genet* **16,** 391-394.

Ruas JL, White JP, Rao RR, Kleiner S, Brannan KT, Harrison BC, Greene NP, Wu J, Estall JL, Irving BA, Lanza IR, Rasbach KA, Okutsu M, Nair KS, Yan Z, Leinwand LA & Spiegelman BM. (2012). A PGC-1alpha isoform

induced by resistance training regulates skeletal muscle hypertrophy. *Cell* **151,** 1319-1331.

Rudnicki MA, Schnegelsberg PN, Stead RH, Braun T, Arnold HH & Jaenisch R. (1993). MyoD or Myf-5 is required for the formation of skeletal muscle. *Cell* **75,** 1351-1359.

Sanchez AM, Csibi A, Raibon A, Cornille K, Gay S, Bernardi H & Candau R. (2012). AMPK promotes skeletal muscle autophagy through activation of forkhead FoxO3a and interaction with Ulk1. *J Cell Biochem* **113,** 695-710.

Sano H, Kane S, Sano E, Miinea CP, Asara JM, Lane WS, Garner CW & Lienhard GE. (2003). Insulin-stimulated phosphorylation of a Rab GTPase-activating protein regulates GLUT4 translocation. *J Biol Chem* **278,** 14599-14602.

Sarabia V, Lam L, Burdett E, Leiter LA & Klip A. (1992). Glucose transport in human skeletal muscle cells in culture. Stimulation by insulin and metformin. *J Clin Invest* **90,** 1386-1395.

Sartori R, Milan G, Patron M, Mammucari C, Blaauw B, Abraham R & Sandri M. (2009). Smad2 and 3 transcription factors control muscle mass in adulthood. *Am J Physiol Cell Physiol* **296,** C1248-1257.

Schiaffino S, Hanzlikova V & Pierobon S. (1970). Relations between structure and function in rat skeletal muscle fibers. *J Cell Biol* **47,** 107-119.

Schiaffino S & Reggiani C. (2011). Fiber types in mammalian skeletal muscles. *Physiol Rev* **91,** 1447-1531.

Seto JT, Lek M, Quinlan KG, Houweling PJ, Zheng XF, Garton F, MacArthur DG, Raftery JM, Garvey SM, Hauser MA, Yang N, Head SI & North KN. (2011). Deficiency of alpha-actinin-3 is associated with increased susceptibility to contraction-induced damage and skeletal muscle remodeling. *Hum Mol Genet* **20,** 2914-2927.

Seto JT, Quinlan KG, Lek M, Zheng XF, Garton F, Macarthur DG, Hogarth MW, Houweling PJ, Gregorevic P, Turner N, Cooney GJ, Yang N & North KN. (2013). ACTN3 genotype influences muscle performance through the regulation of calcineurin signaling. *J Clin Invest* **123,** 4255-4263.

Shang X, Huang C, Chang Q, Zhang L & Huang T. (2010). Association between the ACTN3 R577X polymorphism and female endurance athletes in China. *Int J Sports Med* **31,** 913-916.

Sjostrom L, Lindroos AK, Peltonen M, Torgerson J, Bouchard C, Carlsson B, Dahlgren S, Larsson B, Narbro K, Sjostrom CD, Sullivan M & Wedel H. (2004). Lifestyle, diabetes, and cardiovascular risk factors 10 years after bariatric surgery. *N Engl J Med* **351,** 2683-2693.

Stratford S, Hoehn KL, Liu F & Summers SA. (2004). Regulation of insulin action by ceramide: dual mechanisms linking ceramide accumulation to the inhibition of Akt/protein kinase B. *J Biol Chem* **279,** 36608-36615.

Szendroedi J, Yoshimura T, Phielix E, Koliaki C, Marcucci M, Zhang D, Jelenik T, Muller J, Herder C, Nowotny P, Shulman GI & Roden M. (2014). Role of diacylglycerol activation of PKCtheta in lipid-induced muscle insulin resistance in humans. *Proc Natl Acad Sci U S A* **111,** 9597-9602.

Tack J & Deloose E. (2014). Complications of bariatric surgery: dumping syndrome, reflux and vitamin deficiencies. *Best Pract Res Clin Gastroenterol* **28,** 741-749.

Treebak JT, Glund S, Deshmukh A, Klein DK, Long YC, Jensen TE, Jorgensen SB, Viollet B, Andersson L, Neumann D, Wallimann T, Richter EA, Chibalin AV, Zierath JR & Wojtaszewski JF. (2006). AMPK-mediated AS160 phosphorylation in skeletal muscle is dependent on AMPK catalytic and regulatory subunits. *Diabetes* **55,** 2051-2058.

Tremblay A, Sauve L, Despres JP, Nadeau A, Theriault G & Bouchard C. (1989). Metabolic characteristics of postobese individuals. *Int J Obes* **13,** 357-366.

Tuomilehto J, Lindstrom J, Eriksson JG, Valle TT, Hamalainen H, Ilanne-Parikka P, Keinanen-Kiukaanniemi S, Laakso M, Louheranta A, Rastas M, Salminen V & Uusitupa M. (2001). Prevention of type 2 diabetes mellitus by changes in lifestyle among subjects with impaired glucose tolerance. *N Engl J Med* **344,** 1343-1350.

Vincent B, De Bock K, Ramaekers M, Van den Eede E, Van Leemputte M, Hespel P & Thomis MA. (2007). ACTN3 (R577X) genotype is associated with fiber type distribution. *Physiol Genomics* **32,** 58-63.

Vincent B, Windelinckx A, Van Proeyen K, Masschelein E, Nielens H, Ramaekers M, Van Leemputte M, Hespel P & Thomis M. (2012). Alpha-actinin-3 deficiency does not significantly alter oxidative enzyme activity in fast human muscle fibres. *Acta Physiol (Oxf)* **204,** 555-561.

Vollestad NK, Vaage O & Hermansen L. (1984). Muscle glycogen depletion patterns in type I and subgroups of type II fibres during prolonged severe exercise in man. *Acta Physiol Scand* **122,** 433-441.

Wallberg-Henriksson H & Holloszy JO. (1984). Contractile activity increases glucose uptake by muscle in severely diabetic rats. *J Appl Physiol Respir Environ Exerc Physiol* **57,** 1045-1049.

Wallberg-Henriksson H & Holloszy JO. (1985). Activation of glucose transport in diabetic muscle: responses to contraction and insulin. *Am J Physiol* **249,** C233-237.

Walsh S, Liu D, Metter EJ, Ferrucci L & Roth SM. (2008). ACTN3 genotype is associated with muscle phenotypes in women across the adult age span. *J Appl Physiol (1985)* **105,** 1486-1491.

Wang K, McClure J & Tu A. (1979). Titin: major myofibrillar components of striated muscle. *Proc Natl Acad Sci U S A* **76,** 3698-3702.

Werner ED, Lee J, Hansen L, Yuan M & Shoelson SE. (2004). Insulin resistance due to phosphorylation of insulin receptor substrate-1 at serine 302. *J Biol Chem* **279,** 35298-35305.

White MF, Maron R & Kahn CR. (1985). Insulin rapidly stimulates tyrosine phosphorylation of a Mr-185,000 protein in intact cells. *Nature* **318,** 183-186.

WHO. (2015). Fact Sheet No.312, pp. http://www.who.int/mediacentre/factsheets/fs312/en/.

Wild S, Roglic G, Green A, Sicree R & King H. (2004). Global prevalence of diabetes: estimates for the year 2000 and projections for 2030. *Diabetes Care* **27,** 1047-1053.Wiza C, Chadt A, Blumensatt M, Kanzleiter T, Herzfeld De Wiza D, Horrighs A, Mueller H, Nascimento EB, Schurmann A, Al-Hasani H & Ouwens DM. (2014). Over-expression of PRAS40 enhances insulin sensitivity in skeletal muscle. *Arch Physiol Biochem* **120,** 64-72.

Xiao B, Sanders MJ, Underwood E, Heath R, Mayer FV, Carmena D, Jing C, Walker PA, Eccleston JF, Haire LF, Saiu P, Howell SA, Aasland R,

Martin SR, Carling D & Gamblin SJ. (2011). Structure of mammalian AMPK and its regulation by ADP. *Nature* **472,** 230-233.

Yang N, MacArthur DG, Gulbin JP, Hahn AG, Beggs AH, Easteal S & North K. (2003). ACTN3 genotype is associated with human elite athletic performance. *Am J Hum Genet* **73,** 627-631.

You JS, Lincoln HC, Kim CR, Frey JW, Goodman CA, Zhong XP & Hornberger TA. (2014). The role of diacylglycerol kinase zeta and phosphatidic acid in the mechanical activation of mammalian target of rapamycin (mTOR) signaling and skeletal muscle hypertrophy. *J Biol Chem* **289,** 1551-1563.

Zempo H, Tanabe K, Murakami H, Iemitsu M, Maeda S & Kuno S. (2011). Age Differences in the Relation Between ACTN3 R577X Polymorphism and Thigh-Muscle Cross-Sectional Area in Women. *Genet Test Mol Biomarkers*.

Zhang Y, Nicholatos J, Dreier JR, Ricoult S, Widenmaier SB, Hotamisligil GS, Kwiatkowski DJ & Manning BD. (2014). Coordinated regulation of protein synthesis and degradation by mTORC1. *Nature* **513,** 440-443.

Zurlo F, Larson K, Bogardus C & Ravussin E. (1990). Skeletal muscle metabolism is a major determinant of resting energy expenditure. *J Clin Invest* **86,** 1423-1427.